ASPECTS OF LATE WEICHSELIAN DEGLACIATION IN SOUTH NORWAY: TIMING OF DEGLACIATION, ICE SHEET GEOMETRY, AND CLIMATE VARIATIONS INFERRED FROM SURFACE EXPOSURE AGES OF LATE PLEISTOCENE AND HOLOCENE LANDFORMS

Philipp Marr, Stefan Winkler and Jörg Löffler

With 5 figures and 1 table
Received 8 October 2019 · Accepted 8 November 2019

Summary: The investigation of periglacial and related landforms in South Norway is of great interest for exploring the timing of deglaciation and to assess their geomorphological connectivity to palaeoclimatic changes during the Late Pleistocene and the Holocene. The ice margins of the Scandinavian Ice Sheet during the Last Glacial Maximum (LGM) are reasonably well established. Palaeo-ice thickness can, however, only be estimated by modelling and remains uncertain over large parts of Norway due to sparse field based evidence. Because of the significant influence of the former horizontal and vertical ice-sheet extent on sea-level rise, atmospheric and oceanic circulation patterns, erosive properties of glaciers and ice sheets, englacial thermal boundaries, and deglaciation dynamics, it is crucial to improve the understanding of the topographic properties of the LGM ice sheet. Despite recent progress, there is a lack of terrestrial evidence in the form of numerical age data from South Norway. In this study two high-mountain regions and their surroundings in west (Dalsnibba, 1476 m a.s.l.) and east (Blåhø, 1617 m a.s.l.) South Norway were studied to reconstruct palaeoclimatic conditions and deglaciation patterns. Terrestrial cosmogenic nuclide (^{10}Be) and Schmidt-hammer exposure-age dating (SHD) have been utilized to determine the surface exposure age of glacially transported boulders as well as of boulder-dominated glacial, periglacial, and paraglacial landforms and bedrock outcrops. By developing calibration curves at both study sites for the first time it was possible to obtain landform-age estimates from Schmidt hammer R-(rebound) values. In addition, the formation and stabilization of those landforms and the formative processes have provided indications about the Late Pleistocene and Holocene climate variability and its connectivity to landform development.

Zusammenfassung: Die Untersuchung periglazialer und verwandter Landformen in Südnorwegen ist von großem Interesse, um den Zeitpunkt der Deglaziation zu bestimmen und ihre geomorphologische Konnektivität mit paläoklimatischen Veränderungen während des Spätpleistozäns und des Holozäns zu bewerten. Die Lokationen der Eisränder des skandinavischen Eisschildes während des Letzten Glazialen Maximums (LGM) sind vergleichsweise gut bekannt, die Mächtigkeit des Paläoeises hingegen, welches lediglich modelliert werden kann, bleibt über weite Teile Norwegens angesichts weniger Geländebefunde unklar. Aufgrund des signifikanten Einflusses der früheren horizontalen und vertikalen Ausdehnung des Eisschildes auf den Meeresspiegelanstieg, die atmosphärischen und ozeanischen Zirkulationsmuster, die erosiven Eigenschaften von Gletschern und Eisschilden, die englazialen thermischen Grenzen sowie die Dynamik der Vereisung, ist es entscheidend, die topographischen Strukturen und Eigenschaften des LGM-Eisschildes besser zu verstehen. Trotz der jüngsten Forschungsfortschritte mangelt es in Südnorwegen an terrestrischen Geländebefunden basierend auf numerischen Altersdatierungen. Für diese Arbeit wurden zwei Hochgebirgsregionen und ihre Umgebungen im Westen (Dalsnibba, 1476 m ü.d.M., über dem Meeresspiegel) und Osten (Blåhø, 1617 m ü.d.M.) Südnorwegens zur Rekonstruktion paläoklimatischer Bedingungen und Vergletscherung ausgewählt. Sowohl terrestrische kosmogene Nuklide (^{10}Be) als auch Schmidt-Hammer Expositionsalterdatierung (SHD) wurden angewendet, um die Dauer der Oberflächenexposition von glazial-transportierten Felsblöcken sowie von blockdominierten glazialen, periglazialen und paraglazialen Landformen und anstehendem Festgestein zu bestimmen. Durch die erstmalige Erstellung von Kalibrierungskurven an beiden Untersuchungsstandorten konnten aus Schmidt-Hammer-Rückprallwerten Landform-Altersschätzungen vorgenommen werden. Darüber hinaus konnten die mit der Bildung und Stabilisierung dieser Landformen verbundenen Prozesse nun neue Hinweise auf die spätpleistozäne und holozäne Klimavariabilität und ihre Konnektivität zur Landformentwicklung liefern.

Keywords: Glaciation history, periglacial landforms, landform evolution, surface exposure dating, deglaciation, Norway

1 Introduction

Climate change and the ongoing debates about its consequences are gaining political and public momentum worldwide (Owen et al. 2009; IPCC 2014). Mountain areas, particularly glaciers and ice sheets, respond sensitively to changing climatic conditions. They are currently facing rapid and comprehensive changes with wide-ranging ramifications which are expected to accelerate in the future (Zemp et al. 2008; Barry and Gan 2011; Gobiet et al. 2014; Zemp et al. 2015; Beniston et al. 2018). Glaciers store large amounts of freshwater and their run-off is crucial for irrigation systems as well as hydropower production (Andreassen and Winsvold 2012; Huss et al. 2017). Additionally, they are an integrated part of the global climate system with important effects on global, regional and local environments, e.g. sea-level rise, geomorphological hazards and ecological changes in glacier forelands (Matthews 1992; Kaser et al. 2006; Ballantyne 2018). In this context, diminishing mountain glaciers and ice sheets can be recognized as key components for current and future societal and environmental systems (Zemp et al. 2008; Barry and Gan 2011; IPCC 2014). For the purpose of improving the predictions for future glacier and ice-sheet development together with assessing the consequences of their retreat or disappearance, it is essential to better constrain their (de)glaciation history, past dynamics as well as their influence on landscape evolution (Owen et al. 2009; Hughes et al. 2016; Solomina et al. 2016).

Glacier and ice sheet fluctuations throughout the Quaternary (~2.6 Ma) have had major impacts on environmental conditions and the shape of landscapes worldwide (Böse et al. 2012; Ehlers et al. 2018). During the Last Glacial Maximum (LGM, 26.5–20 ka, Clark et al. 2009) the Eurasian ice-sheet complex represented the third largest ice mass worldwide (Patton et al. 2016), from which the Scandinavian Ice Sheet (SIS) comprised the largest component (Hughes et al. 2016). This qualifies Scandinavian landscapes as potential palaeoclimatic archives for information about (de-)glaciation dynamics together with exploring magnitude and frequency of glacier fluctuations during the LGM and towards the Holocene (see Stroeven et al. 2016). Investigating the late Quaternary glaciation history in Scandinavia, especially in Norway, has attracted the attention of scientists for more than a century (Blytt 1876; Sollid and Sørbel 1994; Mangerud 2004; Andersen et al. 2018a). Knowledge about the former horizontal and vertical extent of glaciers constitutes valuable evidence for a better understanding of palaeo-environmental conditions, such as sea-level changes, atmospheric and oceanic circulation patterns, landform evolution, (de)glaciation dynamics, erosive capacities of ice, englacial thermal boundaries and is crucial for palaeoclimatic, isostatic, and numerical-glaciological modelling (Kutzbach et al. 1998; Linge et al. 2006; Rinterknecht et al. 2006; Hughes et al. 2016; Stroeven et al. 2016). Comprehensive reviews draw a rather clear picture of the SIS margins in Norway throughout different stages within and following the last glaciation (Hughes et al. 2016; Patton et al. 2016, 2017; Stroeven et al. 2016). By contrast, the exact vertical ice extent during this time remains uncertain in large areas, partly because reconstructions were mostly based on isostatic rebound models and not on direct field evidence (Brook et al. 1996; Mangerud 2004; Peltier 2004; Linge et al. 2006; Paus et al. 2006; Goehring et al. 2008).

The diverse landscape in Norway, high mountain areas with isolated summits in south-central and fjord landscapes in southwestern Norway, offers the possibility to explore palaeo-ice thickness conditions (Goehring et al. 2008). Differently weathered landscapes in high mountain areas have been considered as important indicators of Pleistocene ice-sheet dynamics and ice thickness for many years (Dahl 1955; Ballantyne 1998; Briner et al. 2006; McCarroll 2016). The contrast is often apparent in highly weathered uplands, comprising blockfields or tors, and relatively unweathered or freshly exposed glaciated bedrock in lower locations, separated by a trimline (Rea et al. 1996; Goodfellow 2007; Ballantyne 2010). This sometimes well-defined boundary is discussed as a potential indicator of former ice-sheet thickness (Nesje et al. 1988; Linge et al. 2006). Palaeo-ice thickness estimates in Norway range from minimum models with large ice-free areas within a multi-domed ice-sheet configuration (Nesje et al. 1988; Dahl et al. 1997; Follestad 2003), to maximum models suggesting ice cover for most or all summits, alongside a thick SIS (Mangerud 2004; Peltier 2004). For more accurate reconstructions, several concepts are discussed in explaining the appearance of differently weathered mountain landscapes, from which the following two are the most frequently used (e.g. Stroeven et al. 2002). The first scenario implies that highly weathered uplands were ice-free (nunataks) during recent glaciation(s), where the trimline reflected the upper vertical erosional limit of the former ice sheet (e.g. Nesje and Dahl 1990; Rae et al. 2004). Secondly, low-erosive cold-based ice is considered to cover and protect landscape features, where the trimline is regarded as an englacial boundary between warm- and cold-based ice (e.g. Kleman 1994; Stroeven

et al. 2002). Along with a recent paradigm shift towards the latter scenario, there is increasing evidence for a more complex ice sheet during the LGM (Rinterknecht et al. 2006; Mangerud et al. 2010). This requires a critical re-assessment of previous deglaciation chronologies and the role of blockfields and related periglacial landforms as palaeoclimatic proxies (e.g. McCarroll 2016).

The wide application of terrestrial cosmogenic nuclides (TCN) in glacial and periglacial geomorphology revolutionized deglaciation chronologies (Dunai 2010). It largely improved the understanding of the timing of deglaciation and rates of ice thickness degradation (Briner et al. 2006; Linge et al. 2007, Nesje et al. 2007). The importance of periglacial and related landforms as palaeoclimatic proxies is often overlooked despite their potential to provide information on deglaciation and past climate variability (Baumhauer and Winkler 2014; Winkler et al. 2016; Denn et al. 2018; Matthews et al. 2018). These landforms appear to be valuable proxies for past cold periods, as they are considered to have formed during cold climatic conditions and are widespread worldwide (cf. Wilson et al. 2017). However, the formation history and the underlying processes shaping these landforms largely remain ambiguous. Beside the utilisation of TCN in identifying the exposure or burial age of landforms (Fabel et al. 2002; Briner et al. 2006; Nesje et al. 2007), Schmidt-hammer exposure-age dating (SHD) has proved to be appropriate for investigating surface exposure ages by constructing a calibration curve from control points of known age, together with exploring geomorphic processes of boulder-dominated landforms in the periglacial zone (Matthews and Owen 2010; Shakesby et al. 2011; Wilson and Matthews 2016).

Despite the advances in reconstructing former ice-sheet configurations and their implications for landscape evolution as well as the long research tradition (e.g. Nesje et al. 1994b; Goehring et al. 2008; Longva et al. 2009), there is little knowledge about palaeo-ice thickness as well as timing and rates of local deglaciation in South Norway owing to few terrestrial exposure ages (Hughes et al. 2016; Patton et al. 2016). Along with this, Holocene climate variability and its impacts on geomorphological activity often remain elusive (McCarroll and Nesje 1993; Dahl et al. 1997; Goehring et al. 2008; Matthews and Winkler 2011). Deglaciation reconstructions, particularly in the western part of South Norway mostly rely on interpolations of numerical ages from neighbouring areas which require more ground truth data by numerical dating at specific locations. Recent studies on the deglaciation history in Scandinavia (e.g. Hughes et al. 2016; Stroeven et al. 2016) did not provide details of complex local deglaciation histories and mechanisms in South Norway.

In the light of the abovementioned research gaps, we aim to contribute to a better understanding of the timing and rates of local deglaciation and the connectivity between Late Pleistocene as well as Holocene climate variability and landform evolution, based on TCN and SHD investigations in two selected mountain areas in southern Norway. By applying different surface exposure dating methods, it is possible to explore the involved geomorphic processes, together with surface exposure ages which would be not feasible by applying a single method. Opplendskedalen in the Geirangerfjord together with the prominent peak of Dalsnibba is one of the study areas as it is largely unexplored in terms of past climate variability and timing of deglaciation, despite a few studies carried out in Geiranger (Fareth 1987) and its neighbouring fjords (e.g. Rye et al. 1997; Blikra et al. 2006). A beneficial effect of this site is the rather small extent of current glaciers. Their faster response to climatic variability in this maritime setting facilitates detection of smaller changes at higher resolution which would be not possible at larger glaciers (Dahl et al. 2003). At the second study site in eastern South Norway, on the summit of Blåhø, several studies have been carried out dealing with palaeo-ice thickness estimations and deglaciation chronologies (Nesje et al. 1994b; Goehring et al. 2008). This enables us to validate numerical ages from this study with the previously published chronology and to support the existing chronology by new, additional numerical data. The previously published numerical ages from Goehring et al. (2008) enabled construction of a high-precision calibration curve for SHD, ensuring robust surface exposure ages. In order to provide new insights into the mentioned issues, this study focusses on the following four questions:

1) What were the timing and dynamics of local deglaciation in two selected areas of South Norway during and following the Last Glacial Maximum?
2) How did periglacial and related landforms respond to climate variability following the Last Glacial Maximum and during the Holocene?
3) Are periglacial and related landforms potential palaeoclimatic archives which can be explored by the application of Schmidt-hammer exposure-age dating in these areas?
4) What implications do the findings have on the regional deglaciation history?

2 Study areas

The research work presented here focusses on periglacial and related landforms in two high mountain areas in South Norway (Fig. 1). Both research areas are located at 62° latitude north, from the west Norwegian coast eastwards to the Swedish border. The western study area is located around Dalsnibba (1476 m a.s.l.) in Opplendskedalen, near the town of Geiranger in Møre og Romsdal county (62°04'43 N, 7°17'35 E), Breheimen is located south and Reinheimen west of Dalsnibba (see Fig. 1). The topography of the area is characterized by strong elevation gradients within short distances. Dominant landscape features comprise the changes between well-developed glacial valleys and deeply incised fjords as results of repeated glaciations during the Quaternary (Holtedahl 1967; Klemsdal and Sjulsen 1988; Böhme et al. 2015). The smooth landscape between the valleys at higher altitudes (~1800–1500 m a.s.l.) are largely characterized by flat or gently undulated surfaces of pre-glacial origin, also called paleic surfaces (Gjessing 1967; Nesje and Whillans 1994). Moderately weathered, glacially eroded bedrock is widespread at the summit area of Dalsnibba, where a blockfield is absent.

The climate in the western study area is characterized by sub-oceanic conditions, implying a mild periglacial climate with a mean annual air temperature between 0°C and 2°C (1971–2000) and a mean annual precipitation between 2000 and 3000 mm yr^{-1} (http://senorge.no, last accessed: 24. July 2019). Snow depths of more than 5 cm were recorded on 200–350 days from 1971 to 2000 (http://senorge.no, last accessed: 24. July 2019). Permafrost has not been recorded at Dalsnibba. Geologically, the Geiranger region is part of the Norwegian basement which consists of Proterozoic rocks (Sigmond et al. 1984). It is part of the so-called Western Gneiss Region that spans large areas of South Norway and the bedrock consists mainly of quartz dioritic to granitic and is partly migmatitic (Tveten et al. 1998).

There is no detailed deglaciation chronology or palaeo-ice thickness estimation for the western study site, but deglaciation most likely reached the Geirangerfjord during the Bølling–Allerød Interstadial (~14.7–12.9 ka, Patton et al. 2017). During this period glacier dynamics were characterized by several short-term standstills in the fjord (Longva et al. 2009). Glaciers readvanced in the area during the Younger Dryas (YD, ~12.9–11.7 cal. ka BP, Lohne et al. 2013), reflected in the terminal moraines located at the fjord mouth (Longva et al. 2009). According to Fareth (1987) the maximum glacier extent was reached 10.5 ± 0.2 ^{14}C ka BP which subsequently melted rapidly and is thought to have disappeared 500 years later (Longva et al. 2009). Following the YD, the final deglaciation in the fjords in western South Norway is expected to have taken place between 11.2 ± 0.4 and 10.9 ± 0.2 cal. ka BP (cf. Nesje and Dahl 1993, calibrated by Hughes et al. 2016). One of the few palaeo-ice thickness estimations suggested 800–1200 m vertical ice extent in the fjords which became ice-free during the Bølling–Allerød Interstadial (Andersen et al. 1995). However, most of the reconstructions are based on rather old ^{14}C ages which can be problematic and have been questioned in the past (see Donner et al. 1996; Mangerud 2004).

The second study site is located in east South Norway at the summit and surroundings of Blåhø (1617 m a.s.l.) in Ottadalen, close to the town of Vågåmo in Oppland county (61°53'51 N, 9°16'58 E). Blåhø is situated between Rondane in the west, Reinheimen in the north-east and Jotunheimen in the south-east. Gently undulating surfaces dominate the summit area which has a steep slope to the east and gentler gradients to the north and south (Marr et al. 2018). Three lower peaks namely Rundhø (1556 m a.s.l.), Veslrundhø (1514 m a.s.l.) and Storhøi (1455 m a.s.l.) are located west of the summit. An autochthonous blockfield at the summit of Blåhø extends downslope to a trimline at ~1500 m a.s.l. (Nesje et al. 1994b).

The climate is dominated by strong continental conditions. This is reflected in the mean annual air temperature of -2° to -1°C and a mean annual precipitation between 750 and 1000 mm yr^{-1} at the summit (http://senorge.no, last accessed: 24. July 2019) and <500 mm yr^{-1} in valleys which represents one of the driest locations in Norway. A snow depth of >25 cm was recorded at 100–200 days (mean) between 1971 and 2000 at most of the investigated landforms. The sites around Rundhø experienced slightly longer snow accumulation of 200–350 days (http://senorge.no, last accessed: 24. July 2019). At the summit more than 5 cm of snow were measured on 200–350 days, but only on 100–200 days in areas lower than 1000 m a.s.l. (1971–2000) (http://senorge.no, last accessed: 24. July 2019). It is assumed that high wind velocities limit the snow coverage in the summit area. Permafrost measurements by Farbrot et al. (2011) show mean ground temperatures at 5 cm depth of 0.9°C (2008–2009) and 1.0°C (2009–2010) and 0.7°C (September 2008 to August 2010) at 10 cm depth. In the latter period, an active layer thickness of 6 to 7 meters was recorded by Farbrot et al.

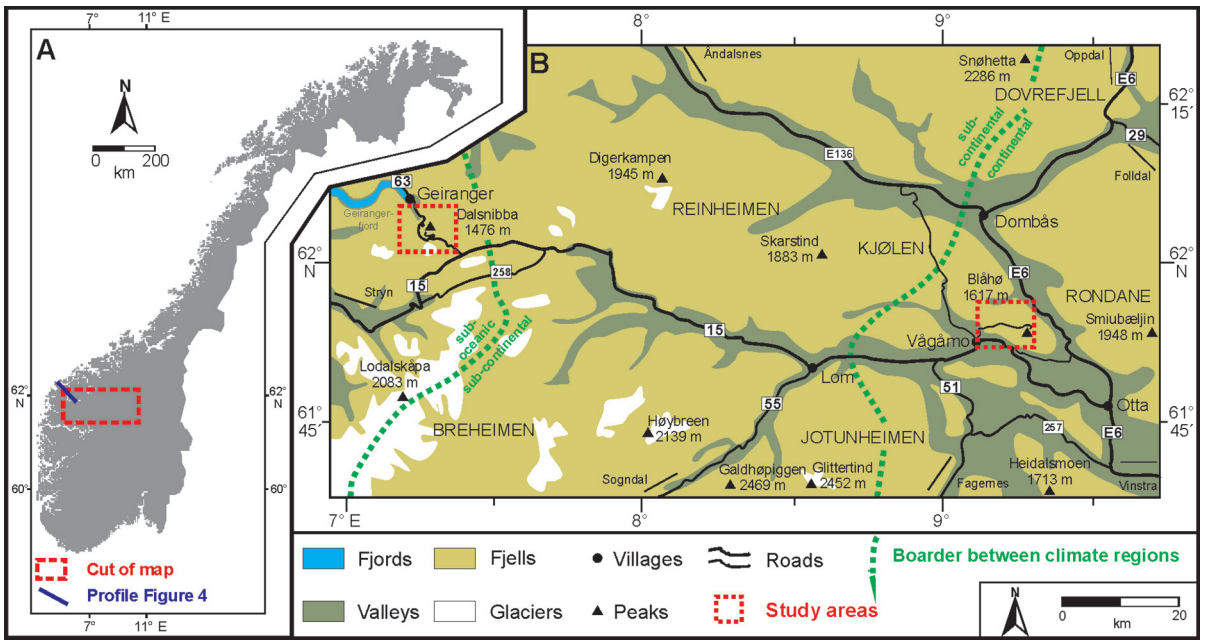

Fig. 1: Study areas in southern Norway with the location of Dalsnibba in the west and Blåhø in the east, marked with red squares (B), their location in Norway and the location of the profile displayed in Figure 4 (A) (modified after Löffler and Pape 2004).

(2011). The area around Blåhø is geologically part of the Kvitola Nappe, comprised of late Precambrian sedimentary rocks (cf. Farbrot et al. 2011). The quartz-rich Precambrian bedrock is present as meta-conglomerate on higher slopes and as meta-sandstone on lower elevations (Tveten et al. 1998).

Blåhø´s deglaciation history is part of an ongoing discussion which focusses on whether the summit was covered by cold-based ice (Goehring et al. 2008) or escaped glaciation as a nunatak (Nesje et al. 1994b). The ^{10}Be based deglaciation chronology of Blåhø was presented along a vertical transect by Goehring et al. (2008) with an erratic boulder from the summit dated to 25.1 ± 1.8 ka (recalculated to 21.8 ± 1.6 ka by Marr et al. (2019b)) which was interpreted as the start of deglaciation. They successively sampled six lower lying glacially transported boulders between 1481–1086 m a.s.l. from which the lowermost sample dates to 11.7 ± 1.0 ka (Goehring et al. 2008). Although the cold-based ice concept is largely accepted by the scientific community (e.g. Fabel et al. 2002), there are indications that it does not apply to all blockfields (McCarroll 2016) and that the glaciation was more dynamic and complex than previously assumed (e.g. Rinterknecht et al. 2006). There is evidence of mountain summits (e.g. Skåla) having escaped glaciation in the vicinity of Blåhø (Brook et al. 1996) which agrees with the assumption that the LGM ice sheet was multi-domed and rather thin (Follestad 2003; Winguth et al. 2005).

3 Research design and methodology

To achieve chronological control of the different periglacial and related landforms, Schmidt-hammer exposure-age dating (SHD) and terrestrial cosmogenic nuclide (TCN) dating were applied. The research design is outlined in Fig. 2.

3.1 Schmidt-hammer exposure-age dating (SHD)

The Schmidt hammer was originally designed to test the in situ concrete hardness of conrete (Schmidt 1950) but has been used in geomorphological research since the 1960s (see Goudie 2006). It was initially utilized for the relative dating of boulder-dominated landforms such as moraines (Winkler 2005), rock glaciers (Humlum 1998) and rock avalanches (Clark and Wilson 2004) and but has since been applied for surface exposure dating (e.g. Shakesby et al. 2006; Matthews and Owen 2010). Schmidt hammer measurements reflect the compressive strength of a rock surface which is assumed to decrease with the degree of rock exposure to subaerial weathering. This allows comparisons between relative surface weathering of boulders, in situations where the factor lithology is uniform (Černá and Engel 2011; Matthews et al. 2013). The rebound (R-) values generated by the electronic Schmidt hammer mirror the rebound velocity of the plunger which is re-

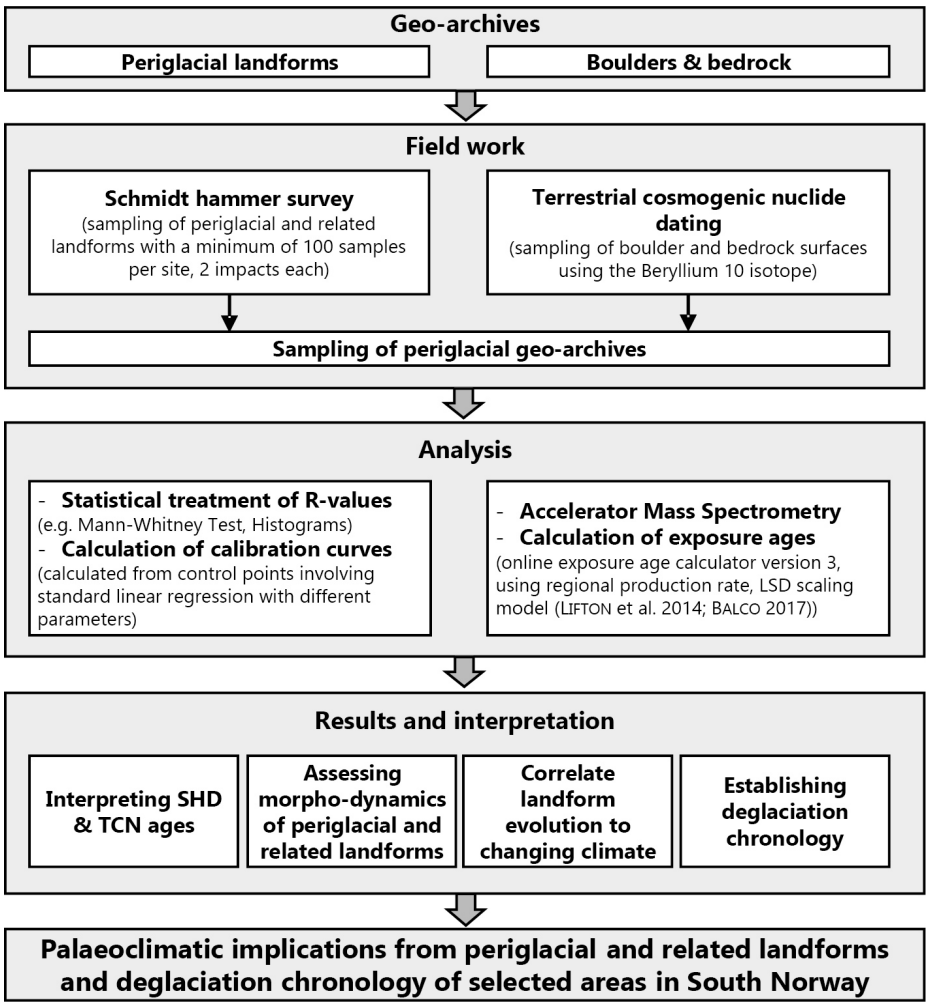

Fig. 2: Research design of this study (modified after BARTZ 2018).

leased on the rock surface (WINKLER and MATTHEWS 2014). Higher R-values are anticipated from freshly exposed rock surfaces. In turn, low R-values are expected from rock surfaces which have experienced long subaerial exposure (MATTHEWS et al. 2013). SHD can estimate surface exposure ages of boulder-related periglacial landforms and allows the dynamics and processes in their formation and stabilization to be assessed utilizing control points of known age to construct a calibration curve (SHAKESBY et al. 2011; MATTHEWS et al. 2014; WILSON and MATTHEWS 2016). This technique was successfully applied in numerous studies on various boulder-dominated landforms in Norway (MATTHEWS et al. 2013; WILSON et al. 2017), United Kingdom (TOMKINS et al. 2016; WILSON and MATTHEWS 2016) and New Zealand (WINKLER 2014). The ages obtained from Schmidt hammer surveys are largely in accordance with findings by radiocarbon dating (e.g. NESJE et al. 1994a), lichenometry (e.g. MATTHEWS and SHAKESBY 1984), optically stimulated luminescence (e.g. STAHL et al. 2013) and TCN (e.g. TOMKINS et al. 2018; WILSON et al. 2019).

3.1.1 Sampling strategy and analyses

Schmidt hammer (electronic RockSchmidt N-Type) measurements were obtained from boulder or bedrock surfaces from different boulder-dominated periglacial and related landforms such as blockfields, rock-slope failures and sorted polygons. From each control point and landform at least 100 and up to 450 boulders and/or bedrock surfaces were measured, each with two impacts per sampled surface. Sampling near rock cracks or edges, structural weaknesses, at lithologically unstable areas or on mosses or lichens were avoided (e.g. SHAKESBY et al. 2011). The rock surfaces were not prepared prior the

measurements as suggested by some studies (for details see Černá and Engel 2011). Micro- and mesotopographic variabilities are expected to average out because of the relatively large sample size (Matthews et al. 2015). Consequently, we consider their influence in our results to be insignificant (Marr et al. 2018). Throughout the SHD studies only stable, near-horizontal boulders with a diameter larger than 30 cm were measured to ensure that measurements from one landform can be treated as a homogenous sample. The influence of potential sources of error on the results other than surface exposure to weathering processes, including microclimatic variability, lithological heterogeneities and post-depositional disturbance have been limited by the relatively large sample sizes (see Winkler 2005, 2009). A similar sampling design was used by Wilson and Matthews (2016) which assures the reliability of the approach and adequate samples sizes (Shakesby et al. 2006; Niedzielski et al. 2009). In sum, in both studies (Marr et al. 2018, 2019a) 3700 boulders with 7400 impacts on 13 periglacial and related landforms were measured.

Standard statistical treatment, such as the calculation of the standard mean, standard error of the mean (SEM), 95% confidence interval, kurtosis, skewness and the Shapiro-Wilk test for normality, was applied to the data. In order to determine the statistical significance between pair of sites the Mann-Whitney test was applied (Marr et al. 2018, 2019a). Landforms with overlapping 95% confidence intervals ($\alpha = 0.05$) were treated as the same population and therefore of the same age (Shakesby et al. 2006). Histograms were created to visualize R-value distributions which can be associated with post-depositional boulder disturbances, incorporation of anomalously old boulders or complex formation histories (McCarroll and Nesje 1993; Wilson and Matthews 2016). As the studied landforms did not show signs of post-depositional disturbance, the SHD ages were interpreted as maximum ages for boulder stabilization and the landform becoming inactive. Beneath all studied landforms older boulders were present, consequently, the SHD ages were treated as minimum ages of landform initiation (Wilson and Matthews 2016).

3.1.2 Age calibration

Age estimations by SHD require a calibration curve, constructed by independently numerically dated control points (Matthews and Owen 2010; Shakesby et al. 2011). Subsequently, it was possible to relate R-values of previously undated surfaces to surface exposure ages. Based on young and old control points, separate calibration equations for the eastern and western part of South Norway have been calculated (for details see Marr et al. 2018, 2019a), from which calibration curves with a standard linear regression have been derived (Matthews and Owen 2010). The accuracy of the age estimates derived by the calibration curves are largely dependent on the reliability of the control sites (Matthews and Owen 2010; Winkler 2014). The estimation of the uncertainties for the SHD ages of the sampling and the control sites were determined by the calculation of the 95% confidence interval (Winkler 2009). The young control point for the high-precision calibration equation at Blåhø was established from a construction site where boulders were 'freshly' exposed to the surface. The old control points were derived from previously ^{10}Be dated bedrock outcrops at Blåhø by Goehring et al. (2008). In order to test the assumption of linear weathering relationship beyond the Holocene towards the Late Glacial (Matthews and Wilson 2015; Winkler and Lambiel 2018) two old control sites have been investigated with ages of 11.4 $\pm$ 1.0 ka and 15.0 $\pm$ 1.1 ka dated by Goehring et al. (2008). In the western study area it was not possible to derive a high-precision calibration equation due to the lack of previously numerically dated rock surfaces suitable for an old control point. Therefore, already existing data from a locality about 50 km north-east of the western study site were utilized (Matthews et al. 2016) due to its lithological similarity to the migmatitic gneiss at Dalsnibba. Following Winkler and Matthews (2014), the R-values from this study were converted as the mechanical Schmidt hammer was used in the study by Matthews et al. (2016). Two young control points were derived from a location next to a construction site at Dalsnibba where 'fresh' boulders were exposed at the surface. The consequences of the application of a local high-precision in the east and a regional calibration curve in the west are discussed in section 4.3.

Following previously published SHD calibration curves, a linear relationship between R-values and age among the young and old control points have been assumed (Winkler et al. 2016; Wilson et al. 2017). A linear relationship throughout the Holocene and sometimes even beyond has been reported in previous studies (Sánchez et al. 2009; Matthews and Winkler 2011; Tomkins et al. 2016). This is supported by the notion that resistant bedrock (e.g. hard crystalline) types in periglacial environments tend to have slow and practically linear weathering rates throughout the Holocene (Colman 1981; Nicholson 2008).

3.2 Terrestrial cosmogenic nuclides (TCN)

The build-up of cosmogenic nuclides, such as ^{10}Be or ^{26}Al by secondary cosmic rays, has been applied for surface exposure age dating in order to assess the duration of surface exposure near or at the earth´s surface (Balco et al. 2008). The application of TCN in glacial environments to constrain the timing and dynamics of deglaciation relies on multiple assumptions. It is necessary that the samples were uniformly exposed to the surface throughout a single period only. Therefore, any inherited cosmogenic nuclide concentration accumulated prior the last deglaciation is assumed to have been removed by erosional processes (Fabel et al. 2002; Briner et al. 2006). Consequently, the amount of cosmogenic nuclides in a sample exemplifies the past erosive capacity of ice sheets. As the erosive capability of ice sheets is strongly related to the basal ice temperature, it is possible to distinguish between cold- and warm-based ice (low- and high-erosive) reflecting englacial boundaries, or can help to evaluate past ice-thickness of warm-based glaciers (Kleman 1994; Harbor et al. 2006). Furthermore, the sample should not have been influenced by burial, erosion or snow shielding (Stroeven et al. 2002; Briner et al. 2006). In this study exposure ages were obtained from a single nuclide (^{10}Be) and were interpreted as minimum ages (Dunai 2010). Details on laboratory procedures and protocols used are given in Marr et al. (2019b).

3.2.1 Research design and age calculation

The aim at the western study site was to establish the first local deglaciation chronology and to gain information on the erosional and thermal properties of the palaeo-ice sheet. By sampling both bedrock and a glacially transported boulder lying on top of glacially modified bedrock, it is potentially possible to obtain this information (Fabel et al. 2002; Heymann et al. 2011). Therefore, four bedrock sites and one glacially transported boulder were sampled. The bedrock samples were obtained from glacially eroded bedrock surfaces from four different elevations between 1476 m a.s.l. to 1334 m a.s.l. (for details see Marr et al. 2019b). The original plan to sample a vertical transect from the summit to the valley bottom of the proximal Opplendskedalen down to ~1050 m a.s.l. had to be modified due to limited accessibility or unsuitable site conditions. The glacially transported boulder showed similar lithological properties to those present on Dalsnibba, and was seated on a glacially eroded bedrock surface in the summit area (Marr et al. 2019b). The samples from Blåhø add two new exposure ages to the existing deglaciation chronology from Goehring et al. (2008). One sample was obtained from a bedrock outcrop from the summit of Blåhø, in proximity to one erratic boulder sitting on the blockfield. Generally, with this limited dataset conclusive statements about the deglaciation history at Blåhø and identifying potential outliers as well as geological bias were not feasible (Stroeven et al. 2016). However, the ages provide valuable new insights into the erosive capacity of the ice sheet and help to validate numerical ages from the previous deglaciation chronology (Goehring et al. 2008).

Age calculations were carried out with the online exposure age calculator version 3, formerly known as the CRONUS-Earth online exposure age calculator (Balco et al. 2008; Balco 2017, http://hess.ess.washington.edu/). The ages further discussed below were calculated with an assumed erosion of 1 mm ka^{-1} and without shielding by snow, vegetation or sediment. Post-glacial glacio-isostatic rebound was considered in the calculation with an uplift of 30 m for Dalsnibba and 100 m for Blåhø (for details see Marr et al. 2019b).

4 Results and discussion

The main results of this synthesis are presented together with the research context of the publications. Linking the findings from Marr et al. (2018, 2019a, 2019b) allows us to reconstruct the (de)glaciation history on Dalsnibba and Blåhø following the LGM as well as to establish deglaciation scenarios on the basis of exposure ages and morphodynamic implications of periglacial and related landforms. Applying consistent methodology in both study areas ensures comparable results and opens the possibility to integrate them in a wider context.

4.1 Dalsnibba

The surfaces exposure ages offer the opportunity to construct the first deglaciation chronology of Opplendskedalen and the summit of Dalsnibba. The anomalously old boulder age (16.5 ± 0.6 ka) in relation to previous estimates of the timing of deglaciation (Nesje and Dahl 1993) and the bedrock ages from a comparable altitudinal setting (13.3 ± 0.6 to 12.7 ± 0.5 ka) have led to the assumption that the boulder shows cosmogenic nuclide inheritance. Consequently, the

boulder age did not reflect the timing of deglaciation. The bedrock samples did not show inheritance, implying that glacial erosion was sufficient to remove previously accumulated nuclides. High-erosive warm-based ice was most likely responsible for the removal of previously accumulated cosmogenic nuclides in bedrock, which agrees with earlier findings (e.g. Aarseth et al. 1997). The presence of warm-based ice and a palaeo-ice thickness of at least 1476 m a.s.l. at Dalsnibba during the LGM is supported by the deposition of the sampled boulder in the summit area. Accumulation of the inherited cosmogenic nuclides in the boulder could have occurred during transport or by accumulation of deep ^{10}Be production by muons (Briner et al. 2016). However, this is most likely not applicable for these samples as higher elevations sites were not prone to this as neutron produced ^{10}Be production rapidly increases with altitude (Briner et al. 2016). By increasingly slower retreat rates of the SIS (14–12 ka, Hughes et al. 2016) parts of the boulder might already have been exposed to cosmic radiation, whereas the deposition together with the subsequent ice disappearance at the summit took until 13.3 ± 0.6 to 12.7 ± 0.5 ka. These results represent the first minimum palaeo-ice thickness estimation based on terrestrial numerical evidence in this area. They oppose the concept that the ice cover in coastal areas was relatively thin, with possible ice-free high coastal areas (Nesje et al. 1987; Mangerud 2004; Winguth et al. 2005).

Furthermore, it is possible to narrow down the potential window of the timing of deglaciation. According to the uppermost bedrock ages the deglaciation started between 13.3 ± 0.6 to 12.7 ± 0.5 ka. Dalsnibba became ice-free towards the end of Bølling–Allerød Interstadial (14.7–12.9 ka) which corresponds with the estimated deglaciation timing at Storfjord (Longva et al. 2009) and the modelled deglaciation by Hughes et al. (2016). On the basis of the overlap between the bedrock ages and Greenland Interstadial 1a (13.3–12.9 ka, Rasmussen et al. 2014), we suggest that the timing of deglaciation most likely occurred during the latter. Moraines in Sweden suggested a comparable timing of deglaciation (Stroeven et al. 2016) and the timing of glacier retreat at Dalsnibba also overlaps with the latest of the three ice margin fluctuations between 25 and 12 ka (Rinterknecht et al. 2004, 2005, 2006). In the light of this, a rather late ice-free situation on Dalsnibba is suggested within the range of the bedrock ages. Another implication derived by the surface exposure ages is that the summit was most likely ice-free during the YD which is supported by ice-free conditions in nearby mountain plateaus of Dovrefjell (cf. Mangerud 2004).

The bedrock results towards the valley bottom inferred that ice persisted at about 1330 m a.s.l. until 10.3 ± 0.5 ka. It was during this time when final local deglaciation was suggested for the region 11.2 ± 0.4 and 10.9 ± 0.2 cal. ka BP (cf. Nesje and Dahl 1993, calibration from Hughes et al. 2016). Consequently, it is likely that the ice cover at Dalsnibba persisted longer than previously assumed and also longer than in the neighbouring Reinheimen region (11 ± 0.2 ka, Andersen et al. 2018a), except for the possibility that the final deglaciation stage included a sudden ice collapse (Marr et al. 2019b). A longer period of ice cover might be explained by the persistence of a local ice-cap or a glacier readvance during the YD. To comprehensively assess the rate of deglaciation, the evaluation of the surface exposure ages by SHD can be helpful in places where TCN samples could not be obtained. The final deglaciation is thought to have been completed by ~9 ka (Lundqvist and Mejdahl 1995; Nesje et al. 2004; Harbor et al. 2006) or slightly earlier (Fabel et al. 2006), but is largely unkown in the Scandinavian mountains (cf. Hughes et al. 2016). The SHD age of 7.47 ± 0.73 ka indicates a longer residual ice body at the valley bottom. This suggests a thinning rate of ~7.3 cm yr^{-1}, Linge et al. (2007) calculated a comparable rate for an inland location. The origin of the ice body persisting in the valley bottom remains elusive, possibly remnants of the YD readvance survived the following climatic amelioration and covered the area through the short climate deterioration known as the 'Finse Event' (~8.4–8.0 cal. ka BP, Nesje and Dahl 2001). As the 'Finse Event' overlaps with the valley bottom surface exposure age, we propose that Opplendskedalen became ice-free following the 'Finse Event'. This timing seems plausible compared to largely retreating glaciers in Norway and Scandinavia (Nesje 2009; Solomina et al. 2016).

Furthermore, SHD ages and R-value characteristics have the capability to explore the climate variations and periglacial processes during the mid-/late-Holocene at the valley bottom and its surroundings. Most of the studied boulder-related periglacial and related landforms stabilized within the Holocene Thermal Maximum (HTM, ~8.0–5.0 ka, Clark et al. 2009), shortly after the deglaciation of Opplendskedalen. The investigated rock-slope failures (RSFs) mostly stabilized during the HTM which is supported by Böhme et al. (2015) and Hermanns et al. (2017). Climatically induced factors, such as increased cleftwater pressure, permafrost degradation and enhanced freeze-thaw activity, caused by increasing temperatures and precipitation pattern

changes, are considered amongst others, as important triggering mechanisms (e.g. Blikra et al. 2006; McColl 2012; Ballantyne et al. 2013). Most likely, RSFs were related to the interplay of long-term stress release and triggering factors linked to warming climate or subsequent, slow permafrost degradation (Marr et al. 2019a). RSFs occurrences during warm periods were supported by findings from Matthews et al. (2018) from nearby Jotunheimen. This opposes the concept that RSFs occur shortly after local deglaciation (Ballantyne et al. 2014). The interpretation that causes of RSFs were climatically controlled has been strengthened by the conceptual rock-slope failure model developed by Matthews et al. (2018). However, one RSF was recorded which most likely did not occur during a warm phase, implying delayed response to prolonged paraglacial stress release throughout the Holocene by climate variability (Marr et al. 2019a). However, single factors triggering RSFs cannot be identified because they can act in various combinations along different time scales where cause and effect are difficult to distinguish (cf. Marr et al. 2018).

The geomorphological dynamics of the different landforms can be explored by the characterization and distribution of R-values. The non-uniform boulder populations observed at some of the investigated landforms suggest that they share complex diachronous formation histories (Marr et al. 2018, 2019a). This was reflected in the broad confidence intervals and platykurtic distribution of the R-values indicating reactivation or reworking of already existing landforms or the continuing supply of debris after the initial event, e.g. at RSFs (see Marr et al. 2019a). Boulder-dominated periglacial landforms are expected to increase in dynamism during cooler climatic conditions (e.g. Ballantyne and Harris 1994; Wilson et al. 2017) and landforms can be reactivated as old, pre-weathered boulders were transported to the surface by frost heave or other processes, leading to negative skewness. Therefore, the mixed age of the pronival rampart can be interpreted as a continuous build-up of the landform most likely since the beginning of the Holocene (Marr et al. 2019a). In contrast to this, a rather uniform boulder population (e.g. RSF-II second fan) suggested that the landform formed during a single event. Due to the high amount of high R-values within the population of RSF-II first fan, it is inferred that the fan was still fed by the rockwall above and that landform formation is still intermittently active even though it appears inactive (Marr et al. 2019a).

4.2 Blåhø

According to the TCN results from Marr et al. (2019b) and the previously published deglaciation chronology from Goehring et al. (2008), two scenarios for the (de)glaciation history for Blåhø are conceivable:

1) The boulder age of 20.9 ± 0.8 ka represents the timing of deglaciation which is broadly in agreement with the recalculated boulder age sampled by Goehring et al. (2008) of 21.8 ± 1.6 ka (Marr et al. 2019b). This appears plausible as ice retreat was suggested after the peak of global ice volume during the LGM between 23–21 ka (Clark et al. 2009). Glacier retreat on Blåhø could be a response to the observed warming at GISP 2 between ~24–21 ka (cf. Goehring et al. 2008). In this scenario, the bedrock age of 46.4 ± 1.7 ka indicates that the summit experienced negligible erosion during the last glaciation. A possible explanation is the coverage by low-erosive cold-based ice protecting the bedrock from glacial erosion which can also explain the inherited cosmogenic nuclide inventory. This scenario is the most favoured option for Blåhø and surroundings for some authors (Kleman and Hättestrand 1999; Boulton et al. 2001; Goehring et al. 2008). Taking into account the ~21 ka of exposure since deglaciation, the bedrock sample is supposed to have been exposed for a cumulative time of ~25 ka prior to deglaciation. Depending on the glaciation history model, it seems possible that the blockfield was exposed since the early Weichselian or the Eem Interglacial according to the time scale from Mangerud (2004).

However, there are indications that this scenario might have to be partly reconsidered. The melting of cold-based ice covering the blockfield would have left geomorphological traces, e.g. meltwater channels cutting through the blockfield (Sollid and Sørbel 1994) which cannot be observed at Blåhø. Additionally, interpreting the trimline as an englacial boundary is not unproblematic as thermal boundaries might be unstable and change frequently, unable to produce a well-defined trimline (Nesje et al. 1987). Nesje and Dahl (1990) point out that the boundary between warm- and cold-based ice are commonly not parallel to the ice surface. Also TCN ages from glacially transported boulders are not unproblematic, age estimations might be erroneous because of post-depositional disturbance or shielding by sediment, following upward migration and surface exposure by upheave (Briner et al. 2006; Heymann et al. 2011). Interestingly, the timing of blockfield stabilization underneath the sampled boulder is determined at ~18 ka, close the inferred

time of boulder deposition (Marr et al. 2018). This could be either explained by rapid thinning of the ice-sheet on Blåhø with both features becoming exposed to the surface at ~4–2 ka apart from each other or the prevailing periglacial (and ice-free) environment with permafrost conditions together with frost-heave processes which have led to the upheave and subsequent boulder deposition. Shortly after this, the blockfield formation has ceased as climate conditions became warmer and the blockfield surface stabilized. In this case the boulder would not reflect the timing of deglaciation but the timing of exhumation. Additionally, it can be ruled out that initial blockfield formation occurred following the deglaciation in scenario 1 because the timing of formation with 4–2 ka is not sufficient (e.g. Ballantyne 2010). Due to the blockfield´s old appearance, subsurface structure (Marr and Löffler 2017), the negative skewness of R-values as well as indications that blockfields probably can date back to the Tertiary (Rea et al. 1996), we suggest that the initial formation began prior the LGM.

2) Assuming that the bedrock nuclide concentration did not involve inherited cosmogenic nuclides, the summit of Blåhø was probably a nunatak during the LGM. The bedrock age corresponds with the Greenland Interstadial 12 (Rasmussen et al. 2014) supporting the possibility that the summit became ice-free during this time and escaped ice-cover since then. Additionally, Wohlfahrt (2010) suggest that the SIS had completely melted away during the early part of MIS 3 (60–45 ka) which alternates with the Bø/Austnes Interstadial (Mangerud et al. 2010) during which parts of Sweden were ice-free (Wohlfahrt 2010). Prolonged ice-free conditions on Blåhø appear to have been possible in the light of the suggested ice-free conditions at nearby Skåla (Brook et al. 1996), model results indicating ice-free locations during the LGM (Winguth et al. 2005) and the unclear Early/Middle Weichselian glaciation history of Norway (Mangerud 2004). Recent findings from Steer et al. (2012) and Andersen et al. (2018b) have inferred that high-elevation low-relief areas in south-central Norway significantly contributed to erosion and were consequently not covered by cold-based low-erosive ice. A nunatak situation is also feasible when considering ice-flow dynamics. Within the first stage the rather thick ice sheet, covered the Norwegian Channel, and transported erratics to Denmark. Subsequently, ice streams developed from the shelf edge upstream, causing major ice thinning further inland (Mangerud 2004). However, due to the limited sample size on Blåhø no conclusive statement about its glaciation history can be made.

SHD ages and R-value characteristics of the different landforms reveal information about climate variations following the LGM. In general, the investigated landforms appear have been inactive with platykurtic R-value distributions and broad confidence intervals indicating complex, long-term formation histories. In the wake of a cold climate event, it has been suggested that boulder-related landforms were (re)activated as they are largely associated with permafrost, often occurring following the local deglaciation (Ballantyne and Harris 1994; Lilleøren et al. 2012). The stabilization of periglacial landforms located above 1450 m a.s.l. could be correlated for the first time with the Karmøy/Bremanger readvance (~18.5–16.5 ka) which has been observed in both western and southern Norway (Winguth et al. 2005; Olsen and Bergstrøm 2007) and has also been detected in an ice advance into the North Sea from the British Ice Sheet (cf. Hughes et al. 2016). Additionally, this cold stage overlaps with Heinrich event I at ~16.8 cal. ka BP (Hemming 2004). Hence, it is striking that the periglacial landforms above 1450 m a.s.l. appear to not have been reactivated by several cold climatic events during the Late Glacial and Holocene. These cold climate events comprise the YD, the 'Erdalen Event' (10.1–9.7 cal. ka BP), the 'Finse Event', the Neoglacial (starting at ~6 ka) and the 'Little Ice Age' just to mention a few (Sejrup et al. 2000; Matthews and Dresser 2008; Nesje 2009). Possibly, the non-reactivation was linked to the structural strength of the landforms, insufficient moisture supply, changes in freeze-thaw conditions and decreasing frost susceptibility of deformable sediment in the inner part of sorted polygons, resulting in the cessation of frost sorting (Winkler et al. 2016; Marr et al. 2018). Important indications for the magnitude of the YD in the area can be derived from the obtained exposure ages. With the deglaciation ages from Goehring et al. (2008) and the landform dynamics by Marr et al. (2018, 2019b) it becomes evident that the summit area has escaped the YD readvance which is supported by Mangerud (2004). Despite the formation of YD moraines close to Blåhø at Lesjakog (Follestad 2007), the summit area escaped re-glaciation. Concerning the palaeo-ice thickness, a rather thin SIS is expected, either due to cold-based ice coverage or the ice-free location on Blåhø and the topographical dependent glaciers in the surrounding valleys.

The Rundhø blockfield, along with the block-stream, stabilized earlier, during the Tampen readvance ~22–19 ka (Sejrup et al. 2009). The stabilization of the sorted polygons at the foot of Rundhø oc-

curred most likely at the beginning of the Karmøy/Bremanger readvance. Both landform stabilizations have been associated with decreasing temperatures and declining moisture supply leading to the termination of frost sorting and heaving processes (cf. Marr et al. 2018). These findings are in contrast to the deglaciation chronology by Goehring et al. (2008) as they have suggested cold-based ice coverage and slow thinning down to ~1450 m a.s.l. at 15.0 ± 1.0 ^{10}Be ka. Based on the results from Marr et al. (2018) a severe periglacial climate without ice coverage since about 19 ka at Rundhø was indicated. Age and characteristics of the RSFs studied around Blåhø have implied that they occurred during warm phases during the Late Glacial and the Holocene (McColl 2012, see section 4.4) and not shortly after deglaciation (Cruden and Hu 1993). For instance, RSF-II appeared to have occurred towards the end of the Bølling–Allerød Interstadial, which is accordance with the Greenland Interstadial 1a (13.3–12.9 ka) (Rasmussen et al. 2014) and overlaps with the deglaciation of Dalsnibba.

4.3 Methodological implications

Connecting the findings from several articles with similar research design offers the possibility to reflect on methodological aspects related to the application of different surface exposure dating techniques. The comparison of the results from SHD applied in this study with similar studies shows that the obtained numerical ages are plausible and reliable (e.g. Matthews and Owen 2010; Shakesby et al. 2011; Winkler et al. 2016). Due to similar SHD sampling strategies (e.g. two impacts per boulder) it is possible to compare calibration curves (Tab. 1, Fig. 3) and results. The most important difference lies between the local high-precision calibration-curve in the eastern and a rather regional calibration curve in the western study area. Problematic about the latter approach was that the old control point had to be derived from a non-local source and can therefore not account for lithological differences present at the initial study site (cf. Marr et al. 2019a). Therefore, it is expected that the age accuracy of the landforms in the western study area was weakened. However, exploring the uncertainties involved in the SHD studies shows that the landforms in the west have a mean total uncertainty of 0.64 ka, the eastern landforms of 0.92 ka. This difference can most likely be explained by the landform ages itself. The landforms from the west were of mid-/late-Holocene age and generally exhibited lower R-value uncertainties, because lithological inhomogeneities usually become more pronounced with time, as evident in the landforms from the east (see Matthews et al. 2013). There, the landforms have higher standard deviations and confidence intervals. Significant difference of the estimated landform ages based on the different calibration curve calculations cannot be observed. The age error seems to be negligible in comparison with statistical and other inaccuracies involving SHD as also shown by Matthews et al. (2014). Further, it was shown in a previous study that the application of a non-local old control point can be successful (Matthews et al. 2014) and the control point measurements from Wilson et al. (2017) from the similar lithology show comparable results.

For the purpose of improving accuracy, two young control points instead of one were used which were later amalgamated to one control point (Marr et al. 2019a). However, this does not necessarily improve the reliability of the control point compared to the results of Marr et al. (2018). It seems that the amount of boulders measured for the control points

Tab. 1: Schmidt hammer R-values and statistics for the control sites from the western (Marr et al. 2019a) and eastern (Marr et al. 2018) study area. Mean R-values are obtained from the means of two impacts on each boulder, 95% confidence intervals were calculated from the number (n) of sampled boulders.

Control point	Age (in yr)[a]	R-value	σ	95% CI[b]	Kurtosis	Skewness	Boulders (n)
Young (west)	3	70.3	5.22	0.51	-0.37	-0.38	200
Young (east)	1	68.3	4.62	0.45	-0.45	0.52	200
Old (west)	11500	40.3	-	2.4			
Old (east)[c]	11400	49.7	9.84	0.97	-0.81	-0.15	200

[a] Age and R-value from Matthews et al. (2016), the R-value used for the calibration curve was 50.3.

[b] Mean of R-values with 95% confidence intervals ($\alpha = 0.05$).

[c] This is the old control point used in calculating the landform ages at (Marr et al. 2018).

are the key for an accurate determination of a young control point and not the amount of control points. In general, there are only minor differences between the young control points of both studies (Tab. 1). This shows that both approaches are adequate to produce reliable data. Unfortunately, due to the inaccessibility of the raw data from the old control point from Matthews et al. (2016), it was not possible to compare the uncertainties between the old control points. To increase the number of old control points, with each point representing a different age, could be a possible improvement for generating exposure ages with lower uncertainties. Especially, as the application of SHD beyond the Holocene requires reliable old control points as the linearity of calibration curves can decrease with time (Shakesby et al. 2011; Marr et al. 2018).

Both calibration curves are shown in Fig. 3. The young and old control points from both study areas show comparable values with only minor differences (Tab. 1, Fig. 3). This implies that both lithologies have comparable rock strength properties when being 'freshly' exposed and also when being aerially exposed for about 11 ka. The similarities between the young and old control points opens the possibility for testing whether a single control point for both, weathered and unweathered surfaces, could be used as 'regional' control points in a larger areas of similar lithological properties. It is interesting that despite the distance and the lithological variability between the two locations, only minor differences can be observed.

Despite the successful application of the Schmidt hammer in this research its usage is not without obstacles. The SHD age from a moraine in the western study area showed that ages need to be assessed together with geomorphological evidence (Marr et al. 2019a). Ensuring this, problematic SHD ages can be identified and re-evaluated. By integrating these aspects into the interpretation it became clear that the obtained moraine age did not reflect the true landform age, but was an overestimation. This was related to the reworking and reactivation of the landform leading to the exposure of older boulders at the surface. This shows the importance of geomorphological analysis in order to avoid potential misinterpretations by simply relying on numerical surface exposure ages from e.g. TCN (Winkler 2018).

Cosmogenic nuclides have shown to be a valuable tool to explore the deglaciation dynamics, even though a larger sample size would be have been desirable. However, as mentioned above, a straightforward interpretation of the numerical ages without taking into account geomorphological factors can result in misinterpretations (Winkler 2018). The ^{10}Be boulder age from Dalsnibba might be interpreted as the timing of deglaciation, but when considering the sampling location and the ages of the bedrock samples in close proximity, it became clear that the boulder showed cosmogenic nuclide inheritance. Therefore, the bedrock ages from the summit were used to estimate the timing of deglaciation. Constructing the deglaciation chronology with the available samples was challenging as not all parts of the mountain could be sampled to generate a valuable vertical transect with TCN. Hence, SHD ages were partly able to fill this gap which made it possible to construct the deglaciation chronology.

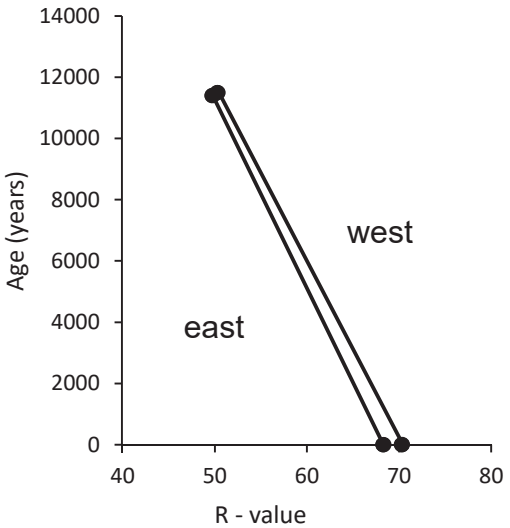

Fig. 3: Calibration curves with old and young control points from the western and eastern study area.

4.4 Implications for the deglaciation history of Southern Norway

This study contributes new aspects to the ongoing discussion about of the deglaciation in South Norway. Exploring the obtained deglaciation chronologies in a regional context, especially in the light of recent deglaciation ages from Reinheimen (Andersen et al. 2018a), located between the study areas, might reveal new insights into regional deglaciation dynamics. Based on the timing of deglaciation from Dalsnibba with 13.3 ± 0.6–12.7 ± 0.5 ka, it appears that the deglaciation in the western part in South Norway has started earlier compared to the assumed timing of deglaciation in Reinheimen at 11 ± 0.2 ka (Andersen et al. 2018a). Accepting that

the boulder age from Blåhø represents the timing of deglaciation (20.9 ± 0.8 ka), the comparison with Reinheimen reveals a divergence of the timing of deglaciation of about 10 ka, even though both areas are at comparable altitudes and only ~30 km apart. The deglaciation at Dalsnibba and Reinheimen have occurred rather late. Hughes et al. (2016) pointed out that the LGM SIS had lost half of its size at the beginning of the Bølling–Allerød Interstadial. This underpins the asynchronous timing of deglaciation in Norway (e.g. Stroeven et al. 2016). The differences in ^{10}Be ages further point to variable basal ice temperatures over a short distance in South Norway. Whereas the ice in the western study area was erosive and warm-based, it appears that the basal temperature properties changed to partly cold-based towards the east as suggested by the results from Andersen et al. (2018a) in Reinheimen. However, they detected only a few bedrock ages showing inheritance.

Because of the proximity to areas investigated by ice-thickness models, it seems valuable to assess the applicability of existing ice-thickness models for Dalsnibba. The ice-thickness model (11–10 km resolution) brought forward by Winguth et al. (2005) for the area of Skåla (~25 km from Dalsnibba) shows an ice thickness of 1100 m a.s.l. at 12.7 ka. Around this time the summit of Dalsnibba was probably already ice-free and the vertical ice extent was ~350 m bigger than on Skåla during this time. Accepting the second Blåhø scenario (section 4.2) with ice-free conditions since about 46 ka, most of the models would overestimate ice-thickness in the south-central Norway during the LGM (e.g. Peltier 2004). Blåhø would stand in line with Skåla, being one of the few nunataks in this area of Norway which could have wide-ranging ramifications for the glaciation history of Scandinavia. However, this scenario has to be tested in more detail in the future.

With the TCN and SHD ages from Dalsnibba, it is now possible to draw a clearer picture of palaeoclimatic conditions from deglaciation into the mid-Holocene (Fig. 4). Summarizing the above-mentioned results and implications, the deglaciation of Dalsnibba took about 5500 years. It started between 13.3 ± 0.6 and 12.7 ± 0.5 ka at the summit and terminated with the valley bottom becoming ice-free shortly after the 'Finse event' around 7.47 ± 0.73 ka. Fig. 4 shows both the aspects which could be answered and which aspects remain elusive. The major problem of integrating the findings of this study to the regional context towards the west are the lack of numerical ages. The deglaciation ages were obtained from the few numerical age constraints from older studies which were based on radiocarbon dating, implying ice-free conditions at 13.5 ± 0.1 ka (Reite 1968, Fig. 4, green star 2, calibrated by Hughes et al. 2016) and deglaciation at 13.8 ± 0.2 ka (Henningsen and Hovden 1984, Fig. 4, green star 3, calibrated by Hughes et al. 2016). Therefore, the deglaciation history of large parts of the area from Dalsnibba towards the sea still remain unclear.

Maritime glaciers have been characterized by a higher mass-turnover than continental glaciers and are therefore anticipated to react faster to cli-

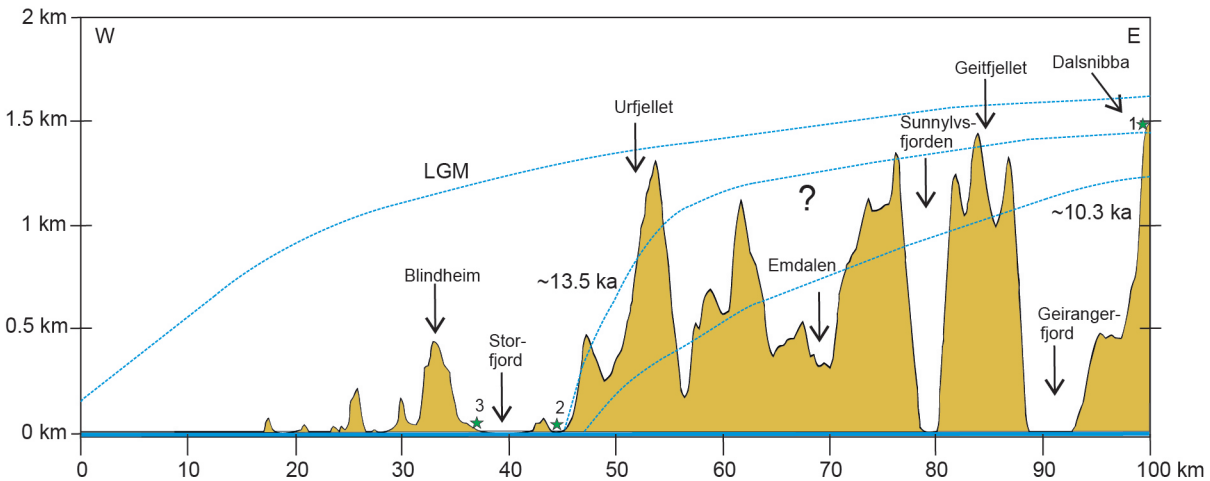

Fig. 4: Topographic model with a west-east profile in western South Norway showing generalized the mountain summits and landform assemblages and the palaeo-ice thickness from the LGM to the early Holocene. The palaeo-ice thickness profile is indicated by the dashed blue line for time slices related to the ^{10}Be ages obtained from Dalsnibba. The location of numerical ages in the area are displayed by green stars, explanations in the text (modified after Gump et al. (2017)). The location of the profile in Norway is displayed in Figure 1.

matic changes (Winkler et al. 2010; Paul et al. 2011; Stroeven et al. 2016). This behaviour is also expected for past glaciations. This could be tentatively demonstrated with the age of the different periglacial and related landforms, as the western landforms reacted more sensitively to climate variability, especially within the Holocene, than those in the eastern study area (Fig. 5). However, it has to be noted that the altitude where the landforms were investigated differed by about 500 m and that in both cases boulder-related periglacial landforms were studied, but not exactly the same landform types. It cannot be ruled out that either younger landforms in the east or older landforms in the west could be found. Nevertheless, the results of the SHD appear to support the notion that western landforms reacted more sensitively to climatic variability. RSFs from both areas occurred during the Bølling–Allerød Interstadial which were probably related to similar climatically induced processes leading to their occurrence (Fig. 5). During warm climatic conditions precipitation changes and increased temperatures led to enhanced snow melt, permafrost degradation causing increased cleft-water pressure, and enhanced freeze-thaw activity which are recognised as potential triggers of RSFs (McColl 2012; Ballantyne et al. 2013; Wilson and Matthews 2016; Marr et al. 2019a).

In sum, this demonstrates that rather small scale interstadials (within the last 130 ka, see Rasmussen et al. 2014) did have a measureable impact on landform evolution. At the same time as the deglaciation started on Dalsnibba, the RSF-II on the foot of Blåhø occurred. This shows that climate variability has differently affected landscape evolution.

5 General conclusions

This geomorphological and geochronological study provides new information on the timing of deglaciation and the response of periglacial and related landforms to climate variability since the Late Quaternary. In general, this study adds to evidence that points to a more complex and dynamic Scandinavian Ice Sheet throughout the last glacial cycle than previously assumed (Rinterknecht et al. 2006; Mangerud et al. 2010). The research was conducted in relation to four research questions and are answered as follows:

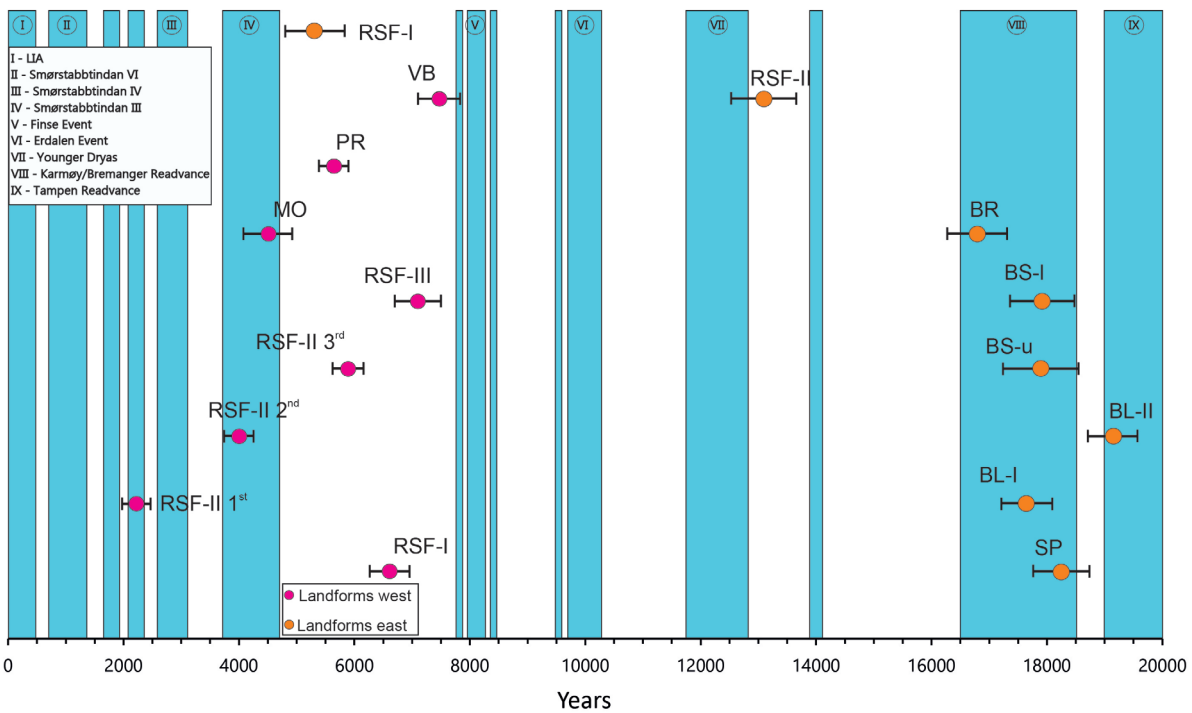

Fig. 5: Plot showing all obtained Schmidt-hammer exposure-age dating results of periglacial and related landforms (Data from Marr et al. (2018, 2019a)). For abbreviations see Marr et al. (2018, 2019a). The exposure ages are plotted with their total error. Major cold climate events from 20 ka towards the present are drawn in blue (data from Nygård et al. 2004; Winguth et al. 2005; Olsen and Bergstrøm 2007; Matthews and Dresser 2008; Sejrup et al. 2009; Lohne et al. 2013).

What were the timing and dynamics of local deglaciation in two selected areas of South Norway during and following the Last Glacial Maximum?

The first deglaciation chronology at Dalsnibba and surroundings in western South Norway shows that the local deglaciation started between 13.3 ± 0.6 to 12.7 ± 0.5 ka. Warm-based ice covered the summit of Dalsnibba during the Last Glacial Maximum up to at least 1476 m a.s.l. The ice subsequently lowered down to the valley bottom of Opplendskedalen, with an average thinning rate of ~7.3 cm yr^{-1}, which became ice-free shortly after the 'Finse event' around ~7.5 ka. In sum, the deglaciation took about 5500 years from summit to valley bottom. Glacier readvances during the Younger Dryas did not reach the summit but most likely reached lower parts of the mountain, resulting in a longer ice persistence than previously assumed.

The timing of local deglaciation at Blåhø could not be finally resolved. Boulders at the summit were exposed to the surface at 20.9 ± 0.8 ka and 21.8 ± 1.6 ka (Goehring et al. 2008, recalculated by Marr et al. 2019b). The process resulting in these exposure ages can be explained by two models. The boulder age either reflects the timing of local deglaciation and the bedrock sample with 46.4 ± 1.7 ka showed inheritance of cosmogenic nuclides. Alternatively, the boulder age represents the timing of exhumation, as it is close the timing of stabilization of the blockfield which was characterized by active geomorphic processes such as frost-heave before its stabilization. Here, the age of the bedrock represents the timing of deglaciation. In this case, the summit was not ice-covered during the Last Glacial Maximum and the boulder age is erroneous due to shielding or reworking. The documented timing of blockfield stabilization on Blåhø requires ice-free conditions which contrasts the inferred ice-coverage at this altitude at that time as suggested by Goehring et al. (2008). Based on this, it is assumed that the previous deglaciation chronology on Blåhø needs to be reconsidered. Together with growing evidence that parts of Greenland and Svalbard were ice-free during large parts of the Pleistocene (Landvik et al. 2003; Schaefer et al. 2016), geomorphic evidence and the inconsistencies of numerical ages, it appears possible that Blåhø has escaped the last glaciation.

It became clear that that there is a strong need for more terrestrial numerical chronological data, especially in western South Norway, to better constrain the timing of deglaciation and ice-sheet characteristics during the Last Glacial Maximum. Therefore, an increase in surface exposure age data could be vital, e.g. vertical transects from summit to fjord bottom. Due to the problems involving cosmogenic nuclides, e.g. post-depositional disturbance of boulders or inheritance (Heymann et al. 2011), other numerical dating techniques such as optically stimulated luminescence from sediment underlying the blockfield should be considered. The application of paired cosmogenic nuclides (e.g. $^{10}Be/^{26}Al$, $^{10}Be/^{21}Ne$) seems to be a possible approach to explore the complex burial history of blockfield surfaces which has not yet been undertaken yet to the knowledge of the authors. In order to improve the understanding of the involved processes operating on present blockfields, the application of InSAR might be helpful to constrain vertical and horizontal displacement rates (Fuhrmann and Garthwaite 2019) and frequencies as shown on permafrost in Svalbard (Rouyet et al. 2019).

How did periglacial and related landforms respond to climate variability following the Last Glacial Maximum and during the Holocene?

In general, periglacial and related landforms respond to climate variability, especially to climate deteriorations. Schmidt-hammer exposure-age dating provided information on the landform dynamics through changing climatic conditions. R-value distributions provided insights into the timing of formation and stabilization of landforms, together with minimum and maximum age estimates from boulder configurations and exposure ages. Most landforms on Blåhø stabilized during the cold climate periods during the Karmøy/Bremanger and Tampen readvances in the Late Glacial. Landform responses to subsequent climate variability could not be reported despite severe cold events following their stabilization in the Holocene, the landforms were not reactivated. Within the western study area, the oldest landform was estimated to have been exposed to the surface since ~7.5 ka. This is significantly later than the exposure ages from the east which implies that western landforms reacted more sensitively to climatic changes, despite the differences of investigated landforms in both areas. It appears that boulder-dominated landforms located in maritime climatic conditions, as in the western study area, reacted more sensitively to Holocene climate variations than the continental influenced eastern landforms. However, landform responses

were not limited to cold climate periods. Rock-slope failures from the western study area indicated that they mostly stabilized during the mid-Holocene coinciding with the Holocene Thermal Maximum. This is generally associated with climate-driven factors, such as permafrost degradation and increasing cleftwater pressure resulting in slope instability. Rock-slope failures in both study areas did not support the concept of higher rock-slope failure frequencies shortly following deglaciation, but they tend to occur during warm periods, several millennials after the local deglaciation. The simultaneous occurrence of deglaciation at Dalsnibba and a rock-slope failure on Blåhø shows that climate variability is affecting the landscape differentially. It could be demonstrated that rather small scale interstadials had a measureable impact on landform evolution.

Are periglacial and related landforms potential palaeoclimatic archives which can be explored by the application of Schmidt-hammer exposure-age dating in these area?

The successful application of Schmidt-hammer exposure-age dating in this study demonstrated that boulder-dominated landforms are an often overseen, but valuable source of palaeoclimatic information. After taking the necessary precautions for accurate sampling locations and strategy, the Schmidt hammer is a strong tool in Late Quaternary dating studies (Wilson et al. 2019). It could be shown that interstadials (e.g. Bølling–Allerød) together with colder climate phases were manifested in distinct landforms in South Norway. For instance, due to Schmidt-hammer exposure-age dating cold climate periods such as the Karmøy/Bremanger readvance could be identified at periglacial landforms located above 1450 m a.s.l. for the first time in the Blåhø area. After the tentative previous reconstructions of the deglaciation reaching the Geirangerfjord, the timing of deglaciation can now be linked to the Bølling–Allerød Interstadial for the first time.

The application of Schmidt-hammer exposure-age dating over larger areas in Norway would be desirable. The Schmidt hammer is a cost and time efficient, user-friendly instrument and with conscious utilization it is possible to obtain a large dataset within a relatively short time. The similarity of both calibration curves, despite their spatial and lithological differences showed that the possibility of regional calibration curves should be considered in the future. Already published calibration curves could be utilized in areas with similar lithological properties, therefore, the construction of single calibration curves for each study site would become obsolete. A potential future research prospect is to construct and test the application of a regional calibration curve for larger areas in southern Norway with similar or comparable lithology. However, the regional lithological variations might become obvious when sampling older surfaces causing significant differences between Younger Dryas and Preboreal surfaces (Shakesby et al. 2006). It is necessary to be aware of the detailed lithological differences and to explore their impact on the precision and accuracy of age estimates.

Which implications do the findings on the regional deglaciation history?

Reconstructing the timing and rates of deglaciation and processes involved on a local scale are crucial in the wake of a more dynamic Scandinavian Ice Sheet throughout the last glacial cycle. It was demonstrated that deglaciation started earlier in western South Norway in comparison to a nearby location towards the east. The divergence of the timing of deglaciation between the neighbouring Reinheimen area and Blåhø by ~10 ka, when accepting the boulder age as the timing of deglaciation, point to an asynchronous timing of deglaciation, differing basal temperatures and variable ice thickness in South Norway. Considering the glaciation history of Blåhø involved parts of ice-free conditions during the Last Glacial Maximum, this would have consequences on the deglaciation history of the Eurasian Ice Sheet and the palaeo-ice thickness reconstructions from Scandinavia. A relatively thin ice sheet raises questions about the sea-level history during the transition from glacial to interglacial due to imbalances between global ice volume estimates and the sum of suggested ice volumes by glacial rebound histories (cf. Winguth et al. 2005).

In conclusion, this study presents insights into the timing of deglaciation, the involved dynamics as well as the role of periglacial and related Late Pleistocene and Holocene landforms as palaeoclimatic and morphodynamic proxies for two areas is South Norway. Additionally, the results contribute to a wider database of terrestrial numerical deglaciation estimates in the inner mountainous areas of western South Norway. Implementing these findings based on terrestrial sources might help to improve models reconstructing glaciation history in South Norway.

Acknowledgments

We like to thank our colleagues and friends who participated actively in this study, either in field, lab, at the summer schools in Svalbard, and at the office. We also thank the Svare family for hospitality and support during field-work periods in Vågå. Philipp Marr received financial support by the DAAD and by the Friedrich-Ebert-Stiftung, for which he is very grateful. Two anonymous reviewers kindly helped to improve the manuscript.

References

Aarseth, I.; Austbo, P. K. and Risnes, H. (1997): Seismic stratigraphy of Younger Dryas ice-marginal deposits in western Norwegian fjords. In: Norsk Geologisk Tidsskrift 77, 65–85.

Andersen, B. G.; Mangerud, J.; Sørensen, R.; Reite, A.; Sveian, H.; Thoresen, M. and Bergström, B. (1995): Younger Dryas ice-marginal deposits in Norway. In: Quaternary International 28, 147–169. https://doi.org/10.1016/1040-6182(95)00037-J

Andersen, J. L.; Egholm, D. L.; Knudsen, M. F.; Linge, H.; Jansen, J. D.; Goodfellow, B. W.; Pedersen, V. K.; Tikhomirov, D.; Olsen, J. and Fredin, O. (2018a): Pleistocene evolution of a Scandinavian plateau landscape. In: Journal of Geophysical Research: Earth Surface 123, 3370–3387. https://doi.org/10.1029/2018JF004670

Andersen, J. L.; Egholm, D. L.; Knudsen, M. F.; Linge, H.; Jansen, J. D.; Pedersen, V. K.; Nielsen, S. B.; Tikhomirov, D.; Olsen, J.; Fabel, D. and Xu, S. (2018b): Widespread erosion on high plateaus during recent glaciations in Scandinavia. In: Nature Communications 9, 830. https://doi.org/10.1038/s41467-018-03280-2

Andreassen, L. M. and Winsvold, S. H. (2012): Inventory of Norwegian glaciers. Norwegian Water Resources and Energy Directorate (NVE), Oslo, Rapport 38-2012.

Balco, G. (2017): Production rate calculations for cosmic-ray-muon-produced ^{10}Be and ^{26}Al benchmarked against geological calibration data. In: Quaternary Geochronology 39, 150–173. https://doi.org/10.1016/j.quageo.2017.02.001

Balco, G.; Stone, J. O.; Lifton, N. A. and Dunai, T. J. (2008): A complete and easily accessible means of calculating surface exposure ages or erosion rates from ^{10}Be and ^{26}Al measurements. In: Quaternary Geochronology 3, 174–195. https://doi.org/10.1016/j.quageo.2007.12.001

Ballantyne, C. K. (1998): Age and significance of mountain-top detritus. In: Permafrost and Periglacial Processes 9, 327–345. https://doi.org/10.1002/(SICI)1099-1530(199810/12)9:4<327::AID-PPP298>3.0.CO;2-9

– (2010): A general model of autochthonous blockfield evolution. In: Permafrost and Periglacial Processes 21, 289–300. https://doi.org/10.1002/ppp.700

– (2018): Periglacial Geomorphology. Oxford.

Ballantyne, C. K. and Harris, C. (1994): The Periglaciation of Great Britain. Cambridge.

Ballantyne, C. K.; Wilson, P.; Schnabel, C. and Xu, S. (2013): Lateglacial rock slope failures in north-west Ireland: age, causes and implications. In: Journal of Quaternary Science 28, 789–802. https://doi.org/10.1002/jqs.2675

Ballantyne, C. K.; Sandeman, G. F.; Stone, J. O. and Wilson, P. (2014): Rock-slope failure following Late Pleistocene deglaciation on tectonically stable mountainous terrain. In: Quaternary Science Reviews 86, 900–913. https://doi.org/10.1016/j.quascirev.2013.12.021

Barry, R. G. and Gan, T. Y. (2011): The global cryosphere: past, present, future. Cambridge.

Bartz, M. (2018): Quaternary fluvial environments in NE Morocco inferred from geochronological and sedimentological investigations. PhD Thesis. Köln.

Baumhauer, R. and Winkler, S. (2014): Glazialgeomorphologie – Formung der Landoberfläche durch Gletscher. Stuttgart.

Beniston, M.; Farinotti, D.; Stoffel, M.; Andreassen, L. M.; Coppola, E.; Eckert, N.; Fantini, A.; Giacona, F.; Hauck, C.; Huss, M.; Huwald, H.; Lehning, M.; López-Moreno, J. I.; Magnusson, J.; Marty, C.; Morán-Tejéda, E.; Morin, S.; Naaim, M.; Provenzale, A.; Rabatel, A.; Six, D.; Stötter, J.; Strasser, U.; Terzago, S. and Vincent, C. (2018): The European mountain cryosphere: a review of its current state, trends, and future challenges. In: Cryosphere 12, 759–794. https://doi.org/10.5194/tc-12-759-2018

Blikra, L. H.; Longva, O.; Braathen, A.; Anda, E.; Dehls, J. F. and Stalsberg K. (2006): Rock slope failures in Norwegian fjord areas: examples, spatial distribution and temporal pattern. In: Evans, S. G.; Mugnozza, G. S.; Strom, A. and Hermanns, R. L. (eds.): Landslides from massive rock slope failure. Dordrecht, 475–496. https://doi.org/10.1007/978-1-4020-4037-5_26

Blytt, A. (1876): Immigration of the Norwegian Flora. Christiania.

Boulton, G. S.; Dongelmans, P.; Punkari, M. and Broadgate, M. (2001): Palaeoglaciology of an ice sheet through a glacial cycle: the European ice sheet through the Weichselian. In: Quaternary Science Reviews 20, 591–625. https://doi.org/10.1016/S0277-3791(00)00160-8

Böhme, M.; Oppikofer, T.; Longva, O.; Jaboyedoff, M.; Hermanns, R. L. and Derron, M.-H. (2015): Analyses of past and present rock slope instabilities in a fjord valley: implications for hazard estimations. In: Geomor-

phology 248, 464–474. https://doi.org/10.1016/j.geomorph.2015.06.045

Böse, M.; Lüthgens, C.; Lee, J. R. and Rose, J. (2012): Quaternary glaciations of northern Europe. In: Quaternary Science Reviews 44, 1–25. https://doi.org/10.1016/j.quascirev.2012.04.017

Briner, J. P.; Miller, G. H.; Thompson Davis, P. and Finkel, R. C. (2006): Cosmogenic radionuclides from fiord landscapes support differential erosion by overriding ice sheets. In: GSA Bulletin 118, 406–420. https://doi.org/10.1130/B25716.1

Briner, J. P.; Goehring, B. M.; Mangerud, J. and Svendsen, J. I. (2016): The deep accumulation of ^{10}Be at Utsira, southwestern Norway: implications for cosmogenic nuclide exposure dating in peripheral ice sheet landscapes. In: Geophysical Research Letters 43, 9121–9129. https://doi.org/10.1002/2016GL070100

Brook, E. J.; Nesje, A.; Lehman, S. J.; Raisbeck, R. M. and Yiou, F. (1996): Cosmogenic nuclide exposure ages along a vertical transect in western Norway: implications for the height of the Fennoscandian ice sheet. In: Geology 24, 207–210. https://doi.org/10.1130/0091-7613(1996)024<0207:CNEAAA>2.3.CO;2

Černá, B. and Engel, Z. (2011): Surface and sub-surface Schmidt hammer rebound value variation for a granite outcrop. In: Earth Surface Processes and Landforms 36, 170–179. https://doi.org/10.1002/esp.2029

Clark, P. U.; Dyke, A. S.; Shakun, J. D.; Carlson, A. E.; Clark, J.; Wohlfarth, B.; Mitrovica, J. X.; Hostetler, S. W. and McCabe, A. M. (2009): The Last Glacial Maximum. In: Science 325, 710–714. https://doi.org/10.1126/science.1172873

Clark, R. and Wilson, P. (2004): A rock avalanche deposit in Burtness Comb, Lake District, northwest England. In: Geological Journal 39, 419–430. https://doi.org/10.1002/gj.965

Colman, S. M. (1981): Rock-weathering rates as functions of time. In: Quaternary Research 15, 250–264. https://doi.org/10.1016/0033-5894(81)90029-6

Cruden, D. M. and Hu, X. Q. (1993): Exhaustion and steady state models for predicting landslide hazards in the Canadian Rocky Mountains. In: Geomorphology 8, 279–285. https://doi.org/10.1016/0169-555X(93)90024-V

Dahl, E. (1955): Biogeographic and geological indications of unglaciated areas in Scandinavia during the glacial ages. In: Bulletin Geological Society of America 66, 1499–1520. https://doi.org/10.1130/0016-7606(1955)66[1499:BAGIOU]2.0.CO;2

Dahl, S. O.; Nesje, A. and Øvstedal, J. (1997): Cirque glaciers as morphological evidence for a thin Younger Dryas ice sheet in the east-central southern Norway. In: Boreas 26, 161–180. https://doi.org/10.1111/j.1502-3885.1997.tb00850.x

Dahl, S. O.; Bakke, J.; Lie, O. and Nesje, A. (2003): Reconstruction of former glacier equilibrium-line altitudes based on proglacial sites: an evaluation of approaches and selection of sites. In: Quaternary Science Reviews 22, 275–287. https://doi.org/10.1016/S0277-3791(02)00135-X

Denn, A. R.; Biermann, P. R.; Zimmermann, S. R. H.; Caffee, M. W.; Corbett, L. B. and Kirby, E. (2018): Cosmogenic nuclides indicate that boulder fields are dynamic, ancient, multigenerational features. In: The Geological Society of America 28, 4–10. https://doi.org/10.1130/GSATG340A.1

Donner, J. (1996): The early and middle Weichselian interstadials in the central area of the Scandinavian glaciations. In: Quaternary Science Reviews 15, 471–479. https://doi.org/10.1016/0277-3791(96)00002-9

Dunai, T. J. (2010): Cosmogenic nuclides: principles, concepts and applications in the earth surface sciences. Cambridge. https://doi.org/10.1017/CBO9780511804519

Ehlers, J.; Gibbard, P. L. and Hughes, P. D. (2018): Quaternary glaciations and chronology. In: Menzies, J. and van der Meer, J. J. M. (eds.): Past glacial environments. Amsterdam, 77–101. https://doi.org/10.1016/B978-0-08-100524-8.00003-8

Fabel, D.; Stroeven, A. P.; Harbor, J.; Kleman, J.; Elmore, D. and Fink, D. (2002): Landscape preservation under Fennoscandian ice sheets determined from in situ produced ^{10}Be and ^{26}Al. In: Earth and Planetary Science Letters 201, 397–406. https://doi.org/10.1016/S0012-821X(02)00714-8

Fabel, D.; Fink, D.; Fredin, O.; Harbor, J.; Land, M. and Stroeven, A. P. (2006): Exposure ages from relict lateral moraines overridden by the Fennoscandian ice sheet. In: Quaternary Research 65, 136–146. https://doi.org/10.1016/j.yqres.2005.06.006

Farbrot, H.; Hipp, T. F.; Etzelmüller, B.; Isaksen, K.; Ødegård, R. S.; Schuler, T. V. and Humlum, O. (2011): Air and ground temperature variations observed along elevation and continentality gradients in Southern Norway. In: Permafrost and Periglacial Processes 22, 343–360. https://doi.org/10.1002/ppp.733

Fareth, O. W. (1987): Glacial geology of middle and inner Nordfjord, western Norway. Geological Survey of Norway, Technical Report 408. Trondheim.

Follestad, B. A. (2003): Development of minor late-glacial ice domes east of Oppdal, Central Norway. In: Norges geologiske undersøkelse Bulletin 441, 39–49.

– (2007): Lesjaskog 1419 III. Preliminart kvartargeologisk kart M 1:50.000. Norges geologiske undersøkelse.

Fuhrmann, T. and Garthwaite, M. C. (2019): Resolving three-dimensional surface motion with InSAR constraints from multi-geometry data fusion. In: Remote Sensing 11, 241. https://doi.org/10.3390/rs11030241

Gjessing, J. (1967): Norway´s paleic surface. In: Norsk Geologisk Tidsskrift 21, 69–132.

Gobiet, A.; Kotlarski, S.; Beniston, M.; Heinrich, G.; Rajczak, J. and Stoffel, M. (2014): 21st century climate change in the European Alps – a review. In: Science of The Total Environment 493, 1138–1151. https://doi.org/10.1016/j.scitotenv.2013.07.050

Goehring, B. M.; Brook, E. J.; Linge, H.; Raisbeck, G. M. and Yiou, F. (2008): Beryllium-10 exposure ages of erratic boulders in southern Norway and implications for the history of the Fennoscandian Ice Sheet. In: Quaternary Science Reviews 27, 320–336. https://doi.org/10.1016/j.quascirev.2007.11.004

Goodfellow, B. W. (2007): Relict non-glacial surfaces in formerly glaciated landscapes. In: Earth-Science Reviews 80, 47–73. https://doi.org/10.1016/j.earscirev.2006.08.002

Goudie, A. S. (2006): The Schmidt Hammer in geomorphological research. In: Progress in Physical Geography 30, 703–718. https://doi.org/10.1177/0309133306071954

Gump, D. J.; Briner, J. P.; Mangerud, J. and Svendsen, J. I. (2017): Deglaciation of Boknafjorden, south-western Norway. In: Journal of Quaternary Science 32, 80–90. https://doi.org/10.1002/jqs.2925

Harbor, J.; Stroeven, A. P.; Fabel, D.; Clarhäll, A.; Kleman, J.; Li, Y.; Elmore, D. and Fink, D. (2006): Cosmogenic nuclide evidence for minimal erosion across two subglacial sliding boundaries of the late glacial Fennoscandian ice sheet. In: Geomorphology 75, 90–99. https://doi.org/10.1016/j.geomorph.2004.09.036

Hemming, S. R. (2004): Heinrich events: massive late Pleistocene detritus layers of the north Atlantic and their global climate imprint. In: Reviews of Geophysics 42, 1–43. https://doi.org/10.1029/2003RG000128

Henningsen, T. and Hovden, Ø. (1984): Weichsel stratigrafi, deglasiasjon, lokalglasiasjon og strandforskyvning i Alesundområdet. Masters Thesis. Bergen.

Hermanns, R. L.; Schleier, M.; Böhme, M.; Blikra, L. H.; Gosse, J.; Ivy-Ochs, S. and Hilger, P. (2017): Rock-avalanche activity in W and S Norway peaks after the retreat of the Scandinavian ice sheet. In: Mikoš, M.; Vilimek, V.; Yin, Y. and Sassa, K. (eds.): Advancing culture of living with landslides (WLF 2017). Cham, 331–338.

Heymann, J.; Stroeven, A. P.; Harbor J. M. and Caffee, M. W. (2011): Too young or too old: evaluating cosmogenic exposure dating based on an analysis of compiled boulder exposure ages. In: Earth and Planetary Science Letters 302, 71–80. https://doi.org/10.1016/j.epsl.2010.11.040

Holtedahl, H. (1967): Notes on the formation of fjord and fjord-valleys. In: Geografiska Annaler: Series A, Physical Geography 49, 188–203. https://doi.org/10.1080/04353676.1967.11879749

Hughes, A. L. C.; Gyllencreutz, R.; Lohne, Ø. S.; Mangerud, J. and Svendsen, J. I. (2016): The last Eurasian ice sheets – a chronological database and time-slice reconstruction, DATED-1. In: Boreas 45, 1–45. https://doi.org/10.1111/bor.12142

Humlum, O. (1998): Rock glaciers on the Faeroe Islands, the north Atlantic. In: Journal of Quaternary Science 13, 293–307. https://doi.org/10.1002/(SICI)1099-1417(199807/08)13:4<293::AID-JQS370>3.0.CO;2-S

Huss, M.; Bookhagen, B.; Huggel, C.; Jacobsen, D.; Bradley, R. S.; Clague, J. J.; Vuille, M.; Buytaert, W.; Cayan, D. R.; Greenwood, G.; Mark, B. G.; Milner, A. M.; Weingartner, R. and Winder, M. (2017): Toward mountains without permanent snow and ice. In: Earths Future 5, 418–435. https://doi.org/10.1002/2016EF000514

IPCC (2014): Climate change 2013: The physical science basis. Contribution of working group I to the 5th Assessment report of the Intergovernmental Panel on Climate Change. Cambridge.

Kaser, G.; Cogley, J. G.; Dyurgerov, M. B.; Meier, M. F. and Ohmura, A. (2006): Mass balance of glaciers and ice caps: consensus estimates for 1961–2004. In: Geophysical Research Letters 33 (L19501). https://doi.org/10.1029/2006GL027511

Kleman, J. (1994): Preservation of landforms under ice sheets and ice caps. In: Geomorphology 9, 19–32. https://doi.org/10.1016/0169-555X(94)90028-0

Kleman, J. and Hättestrand, C. (1999): Frozen-bed Fennoscandian and Laurentide ice sheets during the Last Glacial Maximum. In: Nature 402, 63–66. https://doi.org/10.1038/47005

Klemsdal, T. and Sjulsen, E. (1988): The Norwegian macrolandforms: definition, distribution and system of evolution. In: Norsk Geologisk Tidsskrift 42, 133–147. https://doi.org/10.1080/00291958808552192

Kutzbach, J.; Gallimore, R.; Harrison, S.; Behling, P.; Selin, R. and Laarif, F. (1998): Climate and biome simulations for the past 21,000 years. In: Quaternary Science Reviews 17, 473–506. https://doi.org/10.1016/S0277-3791(98)00009-2

Landvik, J. Y.; Brook, E. J.; Gualtieri, L.; Raisbeck, G.; Salvigsen, O. and Yiou, F. (2003): Northwest Svalbard during the last glaciation: ice-free areas existed. In: Geology 31, 905–908. https://doi.org/10.1130/G19703.1

Lifton, N.; Sato, T. and Dunai, T. J. (2014): Scaling in situ cosmogenic nuclide production rates using analytical approximations to atmospheric cosmic-ray fluxes. In: Earth and Planetary Science Letters 386, 149–160. https://doi.org/10.1016/j.epsl.2013.10.052

Lilleøren, K. S.; Etzelmüller, B.; Schuler, T. V.; Gisnås, K. and Humlum, O. (2012): The relative age of permafrost – estimation of Holocene permafrost limits in Norway. In: Global and Planetary Change 92–93, 209–223. https://doi.org/10.1016/j.gloplacha.2012.05.016

Linge, H.; Brook, E. J.; Nesje, A.; Raisbeck, G.; Yiou, F. and Clark, H. (2006): In situ ^{10}Be exposure ages from southeastern Norway: implications for the geometry of the Weichselian Scandinavian ice sheet. In: Quaternary Science Reviews 25, 1097–1109. https://doi.org/10.1016/j.quascirev.2005.10.007

Linge, H.; Olsen, L.; Brook, E. J.; Darter, J. R.; Mickelson, D. M.; Raisbeck, G. M. and Yiou, F. (2007): Cosmogenic nuclide surface exposure ages from Nordland, northern Norway: implications for deglaciation in a coast to inland transect. In: Norsk Geologisk Tidsskrift 87, 269–280.

Löffler, J. and Pape, R. (2004): Across scale temperature modelling using a simple approach for the characterization of high mountain ecosystem complexity. In: Erdkunde 58, 331–348. https://doi.org/10.3112/erdkunde.2004.04.04

Lohne, Ø. S.; Mangerud, J. and Birks, H. H. (2013): Precise 14C ages of the Vedde and Saksunarvatn ashes and the Younger Dryas boundaries from western Norway and their comparison with the Greenland Ice Core (GICC05) chronology. In: Journal of Quaternary Science 28, 490–500. https://doi.org/10.1002/jqs.2640

Longva, O.; Blikra, L. H.; and Dehls, J. F. (2009): Rock avalanches: distribution and frequencies in the inner part of Storfjorden, Møre og Romsdal County, Norway, Technical Report 2009.002, Geological Survey of Norway. Trondheim. https://www.ngu.no/upload/Publikasjoner/Rapporter/2009/2009_002.pdf

Lundqvist, J. and Mejdahl, V. (1995): Luminescence dating of the deglaciation in northern Sweden. In: Quaternary International 28, 193–197. https://doi.org/10.1016/1040-6182(95)00031-D

Mangerud, J. (2004): Ice sheets limits in Norway and on the Norwegian continental shelf. In: Ehlers, J. and Gibbard, P. L. (eds.): Quaternary glaciations extent and chronology. Amsterdam, 271–294.

Mangerud, J.; Gulliksen, S. and Larsen, E. (2010): ^{14}C-dated fluctuations of the western flank of the Scandinavian Ice Sheet 45–25 kyr BP compared with Bølling–Younger Dryas fluctuations and Dansgaard–Oeschger events in Greenland. In: Boreas 39, 328–342. https://doi.org/10.1111/j.1502-3885.2009.00127.x

Marr, P. and Löffler, J. (2017): Establishing a multi-proxy approach to alpine blockfield evolution in south-central Norway. In: AUC Geographica 52, 219–236. https://doi.org/10.14712/23361980.2017.18

Marr, P.; Winkler, S. and Löffler, J. (2018): Investigations on blockfields and related landforms at Blåhø (Southern Norway) using Schmidt-hammer exposure-age dating: palaeoclimatic and morphodynamic implications. In: Geografiska Annaler: Series A, Physical Geography 100, 285–306. https://doi.org/10.1080/04353676.2018.1474350

Marr, P.; Winkler, S. and Löffler, J. (2019a): Schmidt-hammer exposure-age dating (SHD) performed on periglacial and related landforms in Opplendskedalen, Geirangerfjellet, Norway: Implications for mid- and late-Holocene climate variability. In: The Holocene 29, 97–109. https://doi.org/10.1177/0959683618804634

Marr, P.; Winkler, S.; Binnie, S. A. and Löffler, J. (2019b): ^{10}Be-based exploration of the timing of deglaciation in two selected areas of southern Norway. In: E&G Quaternary Science Journal 68, 165–176. https://doi.org/10.5194/egqsj-68-165-2019

Matthews, J. A. (1992): The Ecology of recently-deglaciated terrain: a geoecological approach to glacier forelands. Cambridge.

Matthews, J. A. and Shakesby, R. A. (1984): The status of 'Little Ice Age' in southern Norway: a relative-age dating of neoglacial moraines with Schmidt hammer and lichenometry. In: Boreas 13, 333–346. https://doi.org/10.1111/j.1502-3885.1984.tb01128.x

Matthews, J. A. and Dresser, P. Q. (2008): Holocene glacier variation chronology of Smørstabbtindan massif, Jotunheimen, Southern Norway, and the recognition of century- to millennial-scale European Neoglacial Events. In: The Holocene 18, 181–201. https://doi.org/10.1177/0959683607085608

Matthews, J. A. and Owen, G. (2010): Schmidt hammer exposure-age dating: developing linear age-calibration curves using Holocene bedrock surfaces from the Jotunheimen-Jostedalsbreen regions of southern Norway. In: Boreas 39, 105–115. https://doi.org/10.1111/j.1502-3885.2009.00107.x

Matthews, J. A. and Winkler, S. (2011): Schmidt-hammer exposure-age dating (SHD): application to early Holocene moraines and a reappraisal of the reliability of terrestrial cosmogenic-nuclide dating (TCND) at Austanbotnbreen, Jotunheimen, Norway. In: Boreas 40, 256–270. https://doi.org/10.1111/j.1502-3885.2010.00178.x

Matthews, J. A. and Wilson, P. (2015): Improved Schmidt-hammer exposure ages for active and relict pronival ramparts in southern Norway, and their palaeoenvironmental implications. In: Geomorphology 246, 7–21. https://doi.org/10.1016/j.geomorph.2015.06.002

Matthews, J. A.; Nesje, A. and Linge, H. (2013): Relict talus-foot rock glaciers at Øyberget, Upper Ottadalen, Southern Norway: Schmidt hammer exposure ages and palaeoenvironmental implications. In: Permafrost and Periglacial Processes 24, 336–346. https://doi.org/10.1002/ppp.1794

Matthews, J. A.; Winkler, S. and Wilson, P. (2014): Age and origin of ice-cored moraines in Jotunheimen and Breheimen, southern Norway: insights from Schmidt-hammer exposure-age dating. In: Geografiska Annaler: Series A, Physical Geography 96, 531–548. https://doi.org/10.1111/geoa.12046

Matthews, J. A.; McEwen, L. and Owen, G. (2015): Schmidt-hammer exposure-age dating (SHD) of snow-avalanche impact ramparts in Southern Norway: approaches, results and implications for landform age, dynamics and development. In: Earth Surface Processes and Landforms 40, 1705–1718. https://doi.org/10.1002/esp.3746

Matthews, J. A.; Owen, G.; Winkler, S.; Vater, A. E.; Wilson, P.; Mourne, R. W. and Hill, J. L. (2016): A rock-surface microweathering index from Schmidt hammer R-values and its preliminary application to some common rock types in southern Norway. In: Catena 143, 35–44. https://doi.org/10.1016/j.catena.2016.03.018

Matthews, J. A.; Winkler, S.; Wilson, P.; Tomkins M. D.; Dortch, J. M.; Mourne, R. W.; Hill, J. L.; Owen, G. and Vater, A. E. (2018): Small rock-slope failures conditioned by Holocene permafrost degradation: A new approach and conceptual model based on Schmidt-hammer exposure-age dating in Jotunheimen, southern Norway. In: Boreas 47, 1144–1169. https://doi.org/10.1111/bor.12336

McCarroll, D. (2016): Trimline trauma: the wider implications of a paradigm shift in recognising and interpreting glacial limits. In: Scottish Geographical Journal 132, 130–139. https://doi.org/10.1080/14702541.2016.1157203

McCarroll, D. and Nesje, A. (1993): The vertical extent of ice sheets in Nordfjord, western Norway: measuring degree of rock surface weathering. In: Boreas 22, 255–265. https://doi.org/10.1111/j.1502-3885.1993.tb00185.x

McColl, S. T. (2012): Paraglacial rock-slope stability. In: Geomorphology 153–154, 1–16. https://doi.org/10.1016/j.geomorph.2012.02.015

Nesje, A. (2009): Latest Pleistocene and Holocene alpine glacier fluctuations in Scandinavia. In: Quaternary Science Reviews 28, 2119–2136. https://doi.org/10.1016/j.quascirev.2008.12.016

Nesje, A. and Dahl, S. O. (1990): Autochthonous block fields in southern Norway: implications for the geometry, thickness, and isostatic loading of the Late Weichselian Scandinavian ice sheet. In: Journal of Quaternary Science 5, 225–234. https://doi.org/10.1002/jqs.3390050305

– (1993): Lateglacial and Holocene glacier fluctuations and climatic variations in western Norway: a review. In: Quaternary Science Reviews 12, 255–261. https://doi.org/10.1016/0277-3791(93)90081-V

– (2001): The Greenland 8200 cal. yr BP event detected in loss-on-ignition profiles in Norwegian lacustrine sediment sequences. In: Journal of Quaternary Science 16, 155–166. https://doi.org/10.1002/jqs.567

Nesje, A. and Whillans, I. M. (1994): Erosion of Sognefjord, Norway. In: Geomorphology 9, 33–45. https://doi.org/10.1016/0169-555X(94)90029-9

Nesje, A.; Blikra, L. H. and Anda, E. (1994a): Dating rockfall-avalanche deposits from degree of rock-surface weathering by Schmidt-hammer tests: a study from Norangsdalen, Sunnmøre, Norway. In: Norsk Geologisk Tidsskrift 74, 108–113.

Nesje, A.; McCarroll, D. and Dahl, S. O. (1994b): Degree of rock surface weathering as an indicator of ice-sheet thickness along an east–west transect across Southern Norway. In: Journal of Quaternary Science 9, 337–347. https://doi.org/10.1002/jqs.3390090404

Nesje, A.; Dahl, S. O. and Bakke, J. (2004): Were abrupt Lateglacial and early-Holocene climatic changes in northwest Europe linked to freshwater outbursts to the North Atlantic and Arctic Oceans? In: The Holocene 14, 299–310. https://doi.org/10.1191/0959683604hl708fa

Nesje, A.; Anda, E.; Rye, N.; Lien, R.; Hole, P. A. and Blikra, H. (1987): The vertical extent of the Late Weichselian ice sheet in the Nordfjord-Møre area, western Norway. In: Norsk Geologisk Tidsskrift 67, 125–141.

Nesje, A.; Dahl, S. O.; Rye, E. A. and Rye, N. (1988): Block fields in southern Norway: significance for the late Weichselian ice sheet. In: Norsk Geologisk Tidsskrift 68, 149–169.

Nesje, A.; Dahl, S. O.; Linge, H.; Ballantyne, C. K.; McCarroll, D.; Brook, E. J.; Raisbeck, G. M. and Yiou, F. (2007): The surface geometry of the Last Glacial Maximum ice sheet in the Andøya–Skånland region, northern Norway, constrained by surface exposure dating and clay mineralogy. In: Boreas 36, 227–239. https://doi.org/10.1111/j.1502-3885.2007.tb01247.x

Nicholson, D. T. (2008): Rock control in microweathering of bedrock surfaces in a periglacial environment. In: Geomorphology 101, 655–665. https://doi.org/10.1016/j.geomorph.2008.03.009

Niedzielski, T.; Migon, P. and Placek, A. (2009): A minimum sample size required from Schmidt hammer measurements. In: Earth Surface Processes and Landforms 34, 1713–1725. https://doi.org/10.1002/esp.1851

Nygård, A.; Sejrup, H. P.; Haflidason, H.; Cecchie, M. and Ottesen, D. (2004): Deglaciation history of the southwestern Fennoscandian ice sheet between 15 and 13 ^{14}C ka BP. In: Boreas. 33, 1–17. https://doi.org/10.1111/j.1502-3885.2004.tb00992.x

Olsen, L. and Bergstrøm, B. (2007): Glacier variations during the LGM interval in the Karmøy – Jæren district, SW Norway. In: NGF Abstracts and Proceedings 1, 73–74. Trondheim.

Owen, L. A.; Thackray, G.; Anderson, R. S.; Briner, J.; Kaufman, D.; Roe, G.; Pfeffer, W. and Yi, C. (2009): Integrated research on mountain glaciers: current status, priorities and future prospects. In: Geomorphology 20, 158–171. https://doi.org/10.1016/j.geomorph.2008.04.019

Patton, H.; Hubbard, A.; Andreassen, K.; Winsborrow, M. and Stroeven, A. P. (2016): The build-up, configuration, and dynamical sensitivity of the Eurasian ice-sheet complex to Late Weichselian climatic and oceanic forcing. In: Quaternary Science Reviews 154, 97–121. https://doi.org/10.1016/j.quascirev.2016.10.009

Patton, H.; Hubbard, A.; Andreassen, K.; Auriac, A.; Whitehouse, P. L.; Stroeven, A. P.; Shackleton, C.; Winsborrow, M.; Heyman, J. and Hall, A. M. (2017): Deglaciation of the Eurasian ice sheet complex. In: Quaternary Science Reviews 169, 148–172. https://doi.org/10.1016/j.quascirev.2017.05.019

Paul, F.; Andreassen, L. M. and Winsvold, S. H. (2011): A new glacial inventory for the Jostedalsbreen region, Norway, from Landsat TM scenes of 2006 and changes since 1966. In: Annals of Glaciology 52, 153–162. https://doi.org/10.3189/172756411799096169

Paus, A.; Velle, G.; Larsen, J.; Nesje, A. and Lie, Ø. (2006): Lateglacial nunataks in central Scandinavia: biostratigraphical evidence for ice thickness from Lake Flåfattjønn, Tynset, Norway. In: Quaternary Science Reviews 25, 1228–1246. https://doi.org/10.1016/j.quascirev.2005.10.008

Peltier, W. R. (2004): Global glacial isostasy and the surface of the Ice-Age earth: The ICE-5G (VM2) model and GRACE. In: Annual Review of Earth and Planetary Sciences 32, 111–149. https://doi.org/10.1146/annurev.earth.32.082503.144359

Rae, A. C.; Harrison, S.; Mighall, T. and Dawson, A.G. (2004): Periglacial trimlines and nunataks of the Last Glacial Maximum: the gap of Dunloe, southwest Ireland: In: Journal of Quaternary Science 19, 87–97. https://doi.org/10.1002/jqs.807

Rasmussen, S. O.; Bigler, M.; Blockley, S. P.; Blunier, T.; Buchardt, S. L.; Clausen, H. B.; Cvijanovic, I.; Dahl-Jensen, D.; Johnsen, S. J.; Fischer, H.; Gkinis, V.; Guillevic, M.; Hoek, W. Z.; Lowe, J. J.; Pedro, J. B.; Popp, T.; Seierstad, I. K.; Steffensen, J. P.; Svensson, A. M.; Vallelonga, P.; Vinther, B. M.; Walker, M. J. C.; Wheatley, J. J. and Winstrup, M. (2014): A stratigraphic framework for abrupt climatic changes during the last glacial period based on three synchronized Greenland ice-core records: refining and extending the INTIMATE event stratigraphy. In: Quaternary Science Reviews 106, 14–28. https://doi.org/10.1016/j.quascirev.2014.09.007

Rea, B. R.; Whalley, W.; Rainey, M. M. and Gordon, J. E. (1996): Blockfields, old or new? Evidence and implications from some plateaus in northern Norway. In: Geomorphology 15, 109–121. https://doi.org/10.1016/0169-555X(95)00118-O

Reite, A. (1968): Lokalglaciasjon på Sunnmøre. In: Norges Geologiske Undersøkelse 247, 262–287.

Rinterknecht, V. R.; Clark, P. U.; Raisbeck, G. M.; Yiou, F.; Brook, E. J.; Tschudi, S. and Lunkka, J.-P. (2004): Cosmogenic ^{10}Be dating of the Salpausselkä I Moraine in southwestern Finland. In: Quaternary Science Reviews 23, 2283–2289. https://doi.org/10.1016/j.quascirev.2004.06.012

Rinterknecht, V. R.; Marks, L.; Piotrowski, J. A.; Raisbeck, G. M.; Yiou, F.; Brook, E. J. and Clark, P.U. (2005): Cosmogenic ^{10}Be ages on the Pomeranian Moraine, Poland. In: Boreas 34, 186–191. https://doi.org/10.1080/03009480600781982

Rinterknecht, V. R.; Clark, P. U.; Raisbeck, G. M.; Yiou, F.; Brook, E. J.; Marks, L.; Zelčs, V.; Lunkka, J.-P.; Pavlovskaya, I. E.; Piotrowski, J. A. and Raukas, A. (2006): The last deglaciation of the southeastern sector of the Scandinavian Ice Sheet. In: Science 311, 1449–1452. https://doi.org/10.1126/science.1120702

Rouyet, L.; Lauknes, T. R.; Christiansen, H. H.; Strand, S. M. and Larsen, Y. (2019): Seasonal dynamics of a permafrost landscape, Adventdalen, Svalbard, investigated by InSAR. In: Remote Sensing of Environment 231, 111236. https://doi.org/10.1016/j.rse.2019.111236

Rye, N.; Nesje, A.; Lien, R.; Blikra, L. H.; Eikenaes, O.; Hole, P. A. and Torsnes, I. (1997): Glacial geology and deglaciation chronology of the area between inner Nordfjord and Jostedalsbreen – Strynefjellet, western Norway. In: Norsk Geologisk Tidsskrift 77, 51–63.

Sánchez, J. S.; Mosquera, D. F. and Vidal Romaní, J. R. V. (2009): Assessing the age-weathering correspondence of cosmogenic ^{21}Ne dated Pleistocene surfaces by the Schmidt Hammer. In: Earth Surfaces Processes and Landforms 34, 1121–1125. https://doi.org/10.1002/esp.1802

Schaefer, M. J.; Finkel, R. C.; Balco, G.; Alley, R. B.; Caffee, M. W.; Briner, J. P.; Young, N. E.; Gow, A. J. and Schwartz, R. (2016): Greenland was nearly ice-free for extended periods during the Pleistocene. In: Nature 540, 252–255. https://doi.org/10.1038/nature20146

Schmidt, E. (1950): Der Beton-Prüfhammer. Schweizer Baublatt, Zürich 68 (28), 378.

Sejrup, H. P.; Larsen, E.; Landvik, J.; King, E. L.; Haflidason, H. and Nesje, A. (2000): Quaternary glaciations in southern Fennoscandia: evidence from southwestern Norway and the northern North Sea region. In: Quaternary Science Reviews 19, 667–685. https://doi.org/10.1016/S0277-3791(99)00016-5

Sejrup, H. P.; Nygård, A.; Hall, A. M. and Haflidason, H. (2009): Middle and Late Weichselian (Devensian) glaciation history of south-western Norway, North Sea and eastern UK. In: Quaternary Science Reviews 28, 370–380. https://doi.org/10.1016/j.quascirev.2008.10.019

Shakesby, R. A.; Matthews, J. A. and Owen, G. (2006): The Schmidt hammer as a relative-age dating tool and

its potential for calibrated-age dating in Holocene glaciated environments. In: Quaternary Science Reviews 25, 2846–2867. https://doi.org/10.1016/j.quascirev.2006.07.011

Shakesby, R. A.; Matthews, J. A.; Karlén, W. and Los, S. O. (2011): The Schmidt hammer as a Holocene calibrated-age dating technique: testing the form of the R-value-age relationship and defining the predicted age errors. In: The Holocene 21, 615–628. https://doi.org/10.1177/0959683610391322

Sigmond, E. M. O.; Gustavson, M. and Roberts, D. (1984): Berggrunnskart over Norge 1:1 milion. Norges Geologiske Undersøkelse. Trondheim.

Sollid, J. L. and Sørbel, L. (1994): Distribution of glacial landforms in southern Norway in relation to the thermal regime of the last continental ice sheet. In: Geografiska Annaler: Series A, Physical Geography 76, 25–35. https://doi.org/10.2307/521317

Solomina, O. N.; Bradley, R. S.; Jomelli, V.; Geirsdottir, A.; Kaufman, D. S.; Koch, J.; McKay, N. P.; Masiokas, M.; Miller, G.; Nesje, A.; Nicolussi, K.; Owen, L. A.; Putnam, A. E.; Wanner, H.; Wiles, G. and Yang, B. (2016): Glacier fluctuations during the past 2000 years. In: Quaternary Science Reviews 149, 61–90. https://doi.org/10.1016/j.quascirev.2016.04.008

Stahl, T.; Winkler, S.; Quigley, M.; Bebbington, M.; Duffy, B. and Duke, D. (2013): Schmidt hammer exposure-age dating (SHD) of late Quaternary fluvial terraces in New Zealand. In: Earth Surface Processes and Landforms 38, 1838–1850. https://doi.org/10.1002/esp.3427

Steer, P.; Huismans, R. S.; Valla, P. G.; Gac, S. and Herman, F. (2012): Bimodal Plio-Quaternary glacial erosion of fjords and low-relief surfaces in Scandinavia. In: Nature Geoscience 5, 635–639. https://doi.org/10.1038/NGEO1549

Stroeven, A. P.; Fabel, D.; Hättestrand, C. and Harbor, J. (2002): A relict landscape in the centre of Fennoscandian glaciation: cosmogenic radionuclide evidence of tors preserved through multiple glacial cycles. In: Geomorphology 44, 145–154. https://doi.org/10.1016/S0169-555X(01)00150-7

Stroeven, A. P.; Hättestrand, C.; Kleman, J.; Heyman, J.; Fabel, D.; Fredin, O.; Goodfellow, B. W.; Harbor, J. M.; Jansen, J. D.; Olsen, L.; Caffee, M. W.; Fink, D.; Lundqvist, J.; Rosqvist, G. C.; Strömberg, B. and Jansson, K. N. (2016): Deglaciation of Fennoscandia. In: Quaternary Science Reviews 147, 91–121. https://doi.org/10.1016/j.quascirev.2015.09.016

Tomkins, M. D.; Dortch, J. M. and Hughes, P. D. (2016): Schmidt hammer exposure dating (SHED): Establishment and implications for the retreat of the last British Ice Sheet. In: Quaternary Geochronology 33, 46–60. https://doi.org/10.1016/j.quageo.2016.02.002

Tomkins, M. D.; Dortch, J. M.; Hughes, P. D.; Huck, J. J.; Stimson, A. G.; Delmas, M.; Calvet, M. and Pallàs, R. (2018): Rapid age assessment of glacial landforms in the Pyrenees using Schmidt hammer exposure dating (SHED). In: Quaternary Research 90, 26–37. https://doi.org/10.1017/qua.2018.12

Tveten, E.; Lutro, O. and Thorsnes, T. (1998): Geologisk kart over Norge, 1:250,000. Ålesund: Norges Geologiske Undersokelse. Trondheim.

Wilson, P. and Matthews, J. A. (2016): Age assessment and implications of late Quaternary periglacial and paraglacial landforms on Muckish Mountain, northwest Ireland, based on Schmidt-hammer exposure-age dating (SHD). In: Geomorphology 270, 134–144. https://doi.org/10.1016/j.geomorph.2016.07.002

Wilson, P.; Matthews, J. A. and Mourne, R. W. (2017): Relict blockstreams at Insteheia, Valldalen-Talfjorden, Southern Norway: their nature and Schmidt hammer exposure age. In: Permafrost and Periglacial Processes 28, 286–297. https://doi.org/10.1002/ppp.1915

Wilson, P.; Linge, H.; Matthews, J. A.; Mourne, R. W. and Olsen J. (2019): Comparative numerical surface exposure-age dating (^{10}Be and Schmidt hammer) of an early-Holocene rock avalanche at Alstadfjellet, Valldalen, southern Norway. In: Geografiska Annaler: Series A, Physical Geography (online first). https://doi.org/10.1080/04353676.2019.1644815

Winguth, C.; Mickelson, D.; Larsen, E.; Darter, J. R.; Moeller, C. A. and Stalsberg, K. (2005): Thickness evolution of the Scandinavian ice sheet during the late Weichselian in Nordfjord, Western Norway: evidence from ice-flow modeling. In: Boreas 34, 176–185. https://doi.org/10.1111/j.1502-3885.2005.tb01013.x

Winkler, S. (2005): The Schmidt hammer as a relative-age dating technique: potential and limitations of its application on Holocene moraines in Mt Cook National Park, Southern Alps, New Zealand. In: New Zealand Journal of Geology and Geophysics 48, 105–116. https://doi.org/10.1080/00288306.2005.9515102

– (2009): First attempt to combine terrestrial cosmogenic nuclide (^{10}Be) and Schmidt hammer relative-age dating: Strauchon Glacier, Southern Alps, New Zealand. In: Central European Journal of Geosciences 1, 274–290. https://doi.org/10.2478/v10085-009-0026-3

– (2014): Investigation of late-Holocene moraines in the western Southern Alps, New Zealand, applying Schmidt-hammer exposure-age dating. In: The Holocene 24, 48–66. https://doi.org/10.1177/0959683613512169

– (2018): Investigating Holocene mountain glaciations: a plea for the supremacy of glacial geomorphology when reconstructing glacier chronologies (supported by an example from the Southern Alps/New Zealand). In: Erdkunde 72, 215–234. https://doi.org/10.3112/erdkunde.2018.03.04

Winkler, S. and Matthews, J. A. (2014): Comparison of electronic and mechanical Schmidt hammers in the context of exposure-age dating: are Q- and R-values interconvertible? In: Earth Surface Processes and Landforms 39, 1128–1136. https://doi.org/10.1002/esp.3584

Winkler, S. and Lambiel, C. (2018): Age constraints of rock glaciers in the Southern Alps/New Zealand – exploring their palaeoclimatic potential. In: The Holocene 28, 778–790. https://doi.org/10.1177/0959683618756802

Winkler, S.; Chinn, T.; Gärtner-Roer, I.; Nussbaumer, S. U.; Zemp, M. and Zumbühl, H. J. (2010): An introduction to mountain glaciers as climate indicators with spatial and temporal diversity. In: Erdkunde 64, 97–118. https://doi.org/10.3112/erdkunde.2010.02.01

Winkler, S.; Matthews, J. A.; Mourne, R. W. and Wilson, P. (2016): Schmidt-hammer exposure ages from periglacial patterned ground (sorted circles) in Jotunheimen, Norway, and their interpretative problems. In: Geografiska Annaler: Series A, Physical Geography 98, 265–285. https://doi.org/10.1111/geoa.12134

Wohlfarth, B. (2010): Ice-free conditions in Sweden during marine oxygen isotope stage 3? In: Boreas 39, 377–398. https://doi.org/10.1111/j.1502-3885.2009.00137.x

Zemp, M.; Roer, I.; Kääb, A.; Hoelzle, M.; Paul, F. and Haeberli, W. (2008): Global glaciers changes: facts and figures. WGMS/UNEP. Zürich.

Zemp, M.; Frey, H.; Gärtner-Roer, I.; Nussbaumer, S. U.; Hoelzle, M.; Paul, F.; Haeberli, W.; Denzinger, F.; Ahlstrøm, A. P.; Anderson, B.; Bajracharya, S.; Baroni, C.; Braun, L. N.; Cáceres, B. E.; Casassa, G.; Cobos, G.; Dávila, L. R.; Delgado Granados, H.; Demuth, M. N.; Espizua, L.; Fischer, A.; Fujita, K.; Gadek, B.; Ghazanfar, A.; Hagen, J. O.; Holmlund, P.; Karimi, N.; Li, Z.; Pelto, M.; Pitte, P.; Popovnin, V. V.; Portocarrero, C. A.; Prinz, R.; Sangewar, C. V.; Severskiy, I.; Sigurðsson, O.; Soruco, A.; Usubalievm, R. and Vincent, C. (2015): Historically unprecedented global glacier decline in the early 21th century. In: Journal of Glaciology 61, 745–762. https://doi.org/10.3189/2015JoG15J017

Authors

Philipp Marr
Prof. Dr. Jörg Löffler
University of Bonn
Department of Geography
Meckenheimer Allee 166
53115 Bonn
Germany
marr@uni-bonn.de
joerg.loeffler@uni-bonn.de

Prof. Dr. Stefan Winkler
Department of Geography and Geology
University of Würzburg
Am Hubland
97074 Würzburg
Germany
stefan.winkler@uni-wuerzburg.de